West Africa in Rodinia: High quality paleomagnetic pole from the 860 Ma Manso dyke swarm (Ghana)

Paul Yves Jean Antonio, Lenka Baratoux, Ricardo Ivan Ferreira Trindade, Sonia Rousse, Anani Ayite, Cristiano Lana, Mélina Macouin, Emmanuel Williams Kobby Adu, Caroline Sanchez, Marco Antônio Leandro Silva, et al.

West Africa in Rodinia: High quality paleomagnetic pole from the ~860 Ma Manso dyke swarm (Ghana)

Paul Yves Jean Antonio[1,2,*], Lenka Baratoux[2], Ricardo I. F. Trindade[1], Sonia Rousse[2], Ayite Anani[3], Cristiano Lana[4], Mélina Macouin[2], Adu E.W. K.[5], Caroline Sanchez[6], Marco A. L. Silva[4], Anne-Sophie Firmin[2], Carmen I. Martinez-Dopico[7], Arnaud Proietti[8], Prince Ofori Amponsah[5], Patrick Asamoah Sakyi[5]

1. Universidade de São Paulo (USP), Instituto de Astronomia, Geofísica e Ciências Atmosféricas (IAG), Rua do Matão, 1226, Cidade Universitária, 05508-090 São Paulo – SP, Brazil.
2. Université Paul Sabatier (UPS) - Toulouse III, Observatoire Midi-Pyrénées (OMP), Géosciences Environnement Toulouse (GET), 14 Avenue Edouard Belin 31400 Toulouse – France.
3. Ghana Geological Survey Authority, 6, 7th Avenue West Ridge, Box M80, Accra – Ghana.
4. Universidade Federal de Ouro Preto (UFOP), Applied Isotope Research Group, Departamento de Geologia, Escola de Minas, Rua Diogo de Vasconcelos, 122, 35400-000 Ouro Preto – MG, Brazil.
5. Department of Earth Science, School of Physical and Mathematical Sciences, University of Ghana, P.O. Box LG 58, Legon-Accra, Ghana.
6. GEOPS, Université Paris-Sud, CNRS, Université Paris-Saclay, Rue du Belvédère, Bât. 504, 91405Orsay, France.
7. INGEIS- Instituto de Geocronología y Geología Isotópica. Av. Int. Güiraldes, Ciudad Universitaria, Ciudad Autónoma de Buenos Aires – Argentina.
8. Centre de Microcaractérisation Raimond Castaing, 3 Rue Caroline Aigle, 31400 Toulouse – France

*** E-mail address:** paulantonio0931@gmail.com

HIGHLIGHTS

- **Primary origin for the ~860 Ma Manso dyke magnetic remanence confirmed by high magnetic stability and a baked contact test**
- **High-latitude position for West Africa between 915 and 860 Ma.**
- **The new ~860 Ma high-quality paleomagnetic pole for West Africa constrains its position in Rodinia.**
- **Paleomagnetically viable long-lived WABAMGO configuration (West Africa-Baltica-Amazonia-Congo) between ~1200 and 800 Ma.**
- **Closure of Nuna's ocean led to the collision of WABAMGO with Laurentia forming Rodinia.**

ABSTRACT

The paleogeography of the Meso-Neoproterozoic Rodinia supercontinent remains debated partly because many stable cratons still lack reliable paleomagnetic data for this period. A new geochronological and paleomagnetic study was conducted on the NNW-trending Manso dyke swarm of southern West Africa (Ghana) to clarify the position of this unconstrained continent in Rodinia. Two U-Pb apatite ages of 857.2 ± 8.5 Ma and 855 ± 16 Ma agree with one previous baddeleyite age, indicating a ~860 Ma emplacement age for the Manso dykes. A characteristic remanent magnetization (ChRM) was isolated by stable single to pseudo-single domain (SD-PSD) magnetite. Well constrained site mean directions obtained for 13 dykes lead to a mean direction for the Manso dyke swarm of $D_m = 181.9°$, $I_m = -77.2°$ ($N = 13$, $\alpha_{95} = 7.6°$, $k = 30.6$), yielding a paleomagnetic pole at 177.6°E, 28.3°S, ($A_{95} = 12.7°$ $K = 11.6$). Two clusters of opposite inclination pass a reversal test (C-class) and the primary origin is supported by a positive baked contact test, satisfying all the seven R-criteria to provide the first West African Tonian key paleomagnetic pole. This key pole indicates a polar latitude for the West Africa craton was during the emplacement of the ~860 Manso dykes. A compilation of reliable paleomagnetic poles for West Africa, Baltica, Amazonia and Congo-São Francisco cratons suggests that these cratons were together between ~1200 and 800 Ma in a long-lived WABAMGO configuration. We suggest that the collision of this block with Laurentia along the Grenvillian-Sunsás orogens closed the external Nuna Ocean and formed Rodinia by extroversion.

Keywords: West Africa, Neoproterozoic, Tonian, Rodinia, paleomagnetism.

1. INTRODUCTION

The Earth's geodynamics at the Mesoproterozoic–Neoproterozoic transition was marked by the making and unmaking of the Rodinia supercontinent, which duration and configuration are still subject of debate (Condie, 2002; Dalziel, 1997; Evans, 2009; Hoffman, 1991; Li et al., 2013; Li et al., 2008; Meert, 2001; Meert and Torsvik, 2003; Merdith et al., 2017; Moores, 1991; Pisarevsky et al., 2003; Sears and Price, 1978; Wen et al., 2018; Wingate et al., 2002). In all models, Laurentia is considered as the central piece of Rodinia, surrounded by passive margins during the late Neoproterozoic, in a similar way to the place occupied by the African plate during the Phanerozoic (Bond et al., 1984; Hoffman, 1991). Regarding the paleomagnetic database for Rodinia, Laurentia has a substantial number of reliable paleomagnetic poles between ~1270 and 1000 Ma, but the ~1000–800 Ma interval lack of high-quality data (Evans, 2009). Around Laurentia, the models place Baltica along the northeastern coast of Laurentia/Greenland in the northern hemisphere or, as an alternative, in an inverted position (Hartz and Torsvik, 2002). Siberia is considered to be close to Laurentia but its relative orientation and distance are debated (Li et al., 2008; Piper, 2007; Pisarevsky and Natapov, 2003; Sears and Price, 1978; Sears and Price, 2000). The most reported position for Siberia is facing the (present-day) northwest margin of Laurentia (Dalziel, 1997; Hoffman, 1991; Li et al., 2008; Pisarevsky and Natapov, 2003). But an alternative position in the southern hemisphere near the North China craton was also proposed (Evans, 2009). Considered as neighbors in most supercontinents (Columbia, Rodinia and Pangea), these three cratons are defined as the "strange attractors" by Meert (2014). The Amazonia, West Africa and Rio de la Plata cratons are unconstrained by palaeomagnetic data during the ~1000–700 Ma interval, but they are usually placed in proximity to western Laurentia (Evans, 2009). Coherence between these blocks but with slight differences in orientation in different reconstructions led Meert (2014) to call them the "spiritual interlopers". Note that at the peak of Rodinia continental assembly at ~950–850

Ma, only four continents (Baltica, São Francisco, North China, and Siberia) exhibit robust paleomagnetic data (Merdith et al., 2017). This emphasizes the still scarce paleomagnetic database for Rodinia event in its "golden age".

The peak of continental Rodinia assembly precedes a drastic change in paleolatitude from a high-latitude for the Rodinian landmasses to a low-latitude paleogeography, which occurred at ~800 Ma, before its breakup at ~750 Ma (Li et al., 2008). This rotation began after the emplacement of a large superplume beneath the polar landmasses at ~840 Ma, triggering large magmatism and rifting (Li et al., 2003). Recently, some authors argued that these events can be better explained by a Tonian inertial interchange true polar wander (IITPW), but its amplitude, characteristics (single shift or TPW oscillations), and duration are debated (Jing et al., 2019; Li et al., 2004; Maloof et al., 2006; Niu et al., 2016; Swanson-Hysell et al., 2012). From an environmental point of view, no glacial deposits were observed in the landmasses during the polar position of Rodinia at ~950–850 Ma (Li et al., 2013), but more constrained are needed since climatic models depends strongly on the Tonian (1000–720 Ma) paleogeography (Donnadieu et al., 2004). The ~812–790 Ma interval is characterized by the Neoproterozoic Bitter Springs Anomaly (BSA), a large negative $\delta^{13}C$ excursion which can be associated with some indicators of increasing oxygenation of the ocean and atmosphere during the radiation of early eukaryotes (Swanson-Hysell et al., 2015b).

Therefore, a precise and reliable Tonian paleogeography is crucial to understand the impact of the Rodinia supercontinent and the magmatic events it encompasses on the Earth's system. In this contribution, we performed a detailed paleomagnetic study on the ~860 Ma Manso dyke swarm (Baratoux et al., 2019) associated with new U-Pb apatite dating to obtain the first Tonian key pole for West Africa. Our first well constrained West Africa key paleomagnetic pole allows us to propose the existence of a long-lived WABAMGO

juxtaposition between West Africa, Baltica, Amazonia and Congo-São Francisco cratons, which collision with Laurentia leaded to the Apex of Rodina supercontinent.

2. GEOLOGICAL SETTING

The West African Craton is composed of two Proterozoic Shields (Reguibat Shield in the north and Leo-Man Shield in the south) stabilized at about ~2 Ga, and separated by the Upper Proterozoic–Paleozoic sedimentary Taoudeni Basin (Black et al., 1979) (**Fig. 1**). The Ghanaian Paleoproterozoic domain (within the Baoulé-Mossi domain) is composed of an association of granitoids and five northeastern trending greenstone belts (Bole-Nagandi, Bui, Sefwi, Ashanti, and Kibi-Winneba belts from west to east, respectively) (Feybesse et al., 2006) (**Fig. 1**). These greenstones and the associated sedimentary basins were deformed during the ~2100–2000 Ma Eburnean Orogeny (Bonhomme, 1962). These two Proterozoic Shields underlie Meso-Neoproterozoic Basins (Affaton et al., 1991). The older sediments of the Volta basin (Lower Voltaian) in southern Ghana were deposited at ~1000 Ma. The southeastern limit of the Volta basin is bordered by the development of the Dahomeyide belt, the southern extension of the Pan-African belts (Affaton et al., 1991) (**Fig. 1**). These Neoproterozoic events have strongly affected the northern West African Craton, where the sedimentary sequences and dykes are folded and deformed along shear zones in the Anti-Atlas Orogen (**Fig. 1**) (Samson et al., 2004), while the Leo-Man Shield in turn remained stable.

Twenty-six distinct dyke swarms were identified in the West African Craton by aeromagnetic mapping according to their orientation (Jessell et al., 2015). In the Leo-Man Shield, Paleoproterozoic–Mesoproterozoic dykes are represented by the ~1790 Ma Libiri swarm, the ~1790 Korsimoro swarm, and the ~1520 Essakane swarm (Baratoux et al., 2019). Paleomagnetic poles from greenstone rocks and Paleo- to Mesoproterozoic dykes were

previously reported by Piper and Lomax (1973). Two Neoproterozoic dyke swarms from Ghana were recently dated by U-Pb baddeleyite at 915 ± 7 Ma for the N070° Oda dyke swarm, and 867 ± 16 Ma for the N355° Manso dyke swarm (Baratoux et al., 2019) (**Fig. 1**). A younger generation of basaltic dykes was also recognized in the northeastern part of Ghana/southern Burkina Faso with an U-Pb baddeleyite age of 198 ± 16 Ma (Hounde dyke swarm) and was related to the Central Atlantic Magmatic Province (CAMP) (Baratoux et al., 2019).

In this study, we sampled the ~860 Ma NNW-trending Manso dykes and one dyke (GH07) of the ~915 ENE- trending Oda dyke swarm (**Fig. 1**). The Manso dykes have mainly a NNW-direction conjugated to a NNE-direction for some branches of the dyke swarm, and are ~50–100 m to the geophysical signature but their contact with the host rock was not observed in the field. They are fresh, coarse to medium-grained dolerites composed mainly of plagioclase and clinopyroxene (augite) with Fe-Ti oxides. Rare orthopyroxene, altered olivine, baddeleyite, and sulfide were also observed (Baratoux et al., 2019). Fine-grained lamprophyre dykes containing micas and some titanite occur in the Ahafo mine. These Neoproterozoic dykes are undeformed, and they crosscut the Paleoproterozoic basement and Paleoproterozoic regional tectonic structures.

FIGURE 1

3. METHODS

3.1. Sampling

Due to the dense vegetation and the occurrence of a thick (up to ~30m) laterite cover, the outcrops of mafic dykes in Ghana are restricted to the rivers, isolated blocks (**Fig. 2**A, B), and fresh outcrops from mine pits. In March 2019 we sampled 121 oriented cylindrical cores using a portable gasoline-powered rock drill, as well as eight hand-samples in the Ahafo mine pit (Newmont Company), for a total of 16 sites. According to the field orientation, 15 dykes are

from the ~860 Ma NNW-trending Manso dyke swarm and one dyke (GH07) is from the ~915 Ma E-trending Oda dyke swarm (Antonio et al., 2019; Baratoux et al., 2019). The number of samples by site (5-8) were restricted essentially due to agreement with local communities and the mining company. Both cores and hand-samples were oriented using solar and magnetic compasses, and no declination difference was observed. The 16 sites sampled cover a vast geographical area (~41,500 km^2) from the capital Accra in southeast Ghana to Sunyani in the northwest via Cape Coast in the south (**Fig. 1** & site coordinates provided in **Table 1**).

3.2. Geochronology

Two samples (GH05 and GH16) were selected for U-Pb geochronology on apatite. Apatite separation was performed in the Géosciences Environnement Toulouse (GET, France) laboratory. Hand-samples were crushed and sieved to collect the mineral fraction below 400 µm. The low-density minerals and clay fraction were removed using a Wilfley table. Heavy minerals were then isolated using heavy liquids (tetrabromoethane and diiodomethane, with respective densities of 2.967 and 3.325 g/cm^3). Magnetic minerals were consequently removed with a Franz magnetic separator. Finally, the apatite grains were handpicked using a binocular microscope before being mounted into epoxy puck and polished. U-Pb data were acquired at the Isotopic Geochemistry Laboratory in Federal University of Ouro Preto (UFOP, Brazil) using a 193 nm HelEX Photon Machine coupled with a ThermoScientific Neptune Plus Multicollector (LA-MC-ICP-MS). A beam spot size of 85 µm was used with beam energy densities of 6 J/cm^{-2}, and a 6-Hz repetition rate. During apatite U-Pb measurement sequences, the 91500 zircon (Wiedenbeck et al., 1995) was used as a primary reference standard, while the Durango apatite (McDowell et al., 2005), the 401 apatite (Thompson et al., 2016), and the Madagascar apatite (Thomson et al., 2012) were used as secondary reference material in order to correct for matrix match effects as well as to constrain and verify the corrections accuracy and reproducibility. Data reduction and correction was carried out with the SATURN package of the laboratory of

Ouro Preto. Apatite U-Pb ages of the studied samples are reported as isochron ages calculated as lower-intercepts on a Terra-Wasserburg Concordia diagram using the Isoplot 4.15 software (**Fig. 2**) (Ludwig, 2009). The grains analyzed from each sample are igneous co-genetic apatites. Initial common Pb value was anchored to a $^{207}Pb/^{206}Pb$ value of 0.898 (Stacey and Kramers, 1975) according to the U-Pb baddeleyite (ID-TIMS) crystallization age of 867±16 Ma (Baratoux et al., 2019). All the apatite isotopic data, at 2σ level, are reported in the **supplementary material 1**. Additional information on the analytical conditions, and the Terra-Wasserburg Concordia diagrams of reference materials, are provided in the **supplementary material 2**.

3.3. Paleomagnetism

Oriented blocks were drilled in Geosciences Montpellier (France). Preparation of standard specimens (2.2 cm height) and alternating field (AF) demagnetization for a pilot study were carried out at the GET (Toulouse, France) using a JR5-A spinner magnetometer and a LDA-3 AF demagnetizer (AGICO) in a MMLFC shielded room design to reduce the effect of ambient magnetic field (<200 nT). For the remaining samples the characteristic remanent magnetization (ChRM) was isolated by stepwise AF and thermal demagnetization performed in a magnetically shielded room with ambient field <500 nT at the Laboratorio de Paleomagnetismo of the University of São Paulo (USPMag, Brazil). An AF pre-treatment until 10 mT was performed before thermal demagnetization, to eliminate an eventual low-coercivity, viscous component. AF and thermal demagnetizations were performed using a vertical 2G-Enterprises™ DC-SQUID magnetometer with a RAPID automatic sample changer (Kirschvink et al., 2008). Stepwise thermal demagnetization of 50°C (until 500°C) and 20°C (until 700°C) were carried out using a TD-48 furnace device. Only principal component analysis (PCA) (Kirschvink, 1980) was used to determine the remanence directions using orthogonal vector diagrams (Zijderveld, 1967). Site mean directions and paleomagnetic poles were calculated by

Fisher's (1953) statistics using the PALEOMAC package (Cogné, 2003). Paleogeographic reconstructions were performed using the GPlates software (Müller et al., 2018). Magnetic mineralogy was investigated under optical microscopy and using a Scanning Electron Microscopy (SEM JEOL JSM 7100F TTLS LV – EDS/EBSD) at the Centre de Micro Caractérisation Raimond Castaing (Toulouse, France). High-temperature thermomagnetic curves (susceptibility versus temperature) were conducted at the Toulouse, France) in an argon atmosphere using a CS-3 apparatus coupled to the KLY-3 Kappabridge (AGICO, Brno, Czech. Republic). In addition, hysteresis loops, isothermal remanent magnetization (IRM) and first-order reversal curve (FORC) for selected samples were performed at the LABGeo, Instituto Oceanográfico, University of São Paulo (Brazil) using a MicroMag-VSM, Model 3900 (Princeton Measurements Corporation). FORC diagrams were processed using the Forcot software (Berndt and Chang, 2019).

4. RESULTS

4.1. Geochronology

The GH05 site is situated near Cape Coast, between the towns of Yamoransa and Biriwa (southern Ghana) (Fig 1). It is a 20-50m wide dyke disintegrated into several blocks of coarse-grained relatively fresh dolerite, with ~0.5 cm of weathering crust (**Fig. 2**A). The second dated site GH16 is located within the Bechem city (SE of Sunyani) (Fig.1). Multiple blocks of metric size (*in situ*) were observed in an open area (**Fig. 2**B). The dyke is a coarse-grained dolerite showing a fresh doleritic texture (*i.e*. intergranular subophitic).

Apatites from the doleritic samples (GH05 and GH16) exhibit a nearly perfect euhedral prism shape (**Fig. 2**C, D) with grain size ranging between 90 and 300 µm. The isotopic data obtained for the GH05 dolerite sample displays variable proportions of common Pb with

$^{207}Pb/^{206}Pb$ values varying between 0.32 and 0.53. The anchored lower intercept age for this sample is 857.2 ± 8.5 Ma with a MSWD of 2.2 using 17 apatites (**Fig. 2**C). Sample GH16 (dolerite dyke) displays variable proportions of common Pb with $^{207}Pb/^{206}Pb$ values between 0.45 and 0.64. Data for this sample define an anchored lower intercept age of 855 ± 16 Ma with a MSWD of 2.4 using 13 apatites (**Fig. 2**D). The unanchored plots give identical ages for GH05 and GH16 respectively within the error of 841 ± 31 Ma (MSWD = 2.2) and 833 ± 66 Ma (MSWD = 2.5), respectively, but the anchored ages were preferred following Chew et al. (2011).

FIGURE 2

Supplementary material 1

Supplementary material 2

4.2. Paleomagnetic results

Natural remanent magnetization (NRM) values for the dolerite dykes vary between ~0.1 and 9.8 $A.m^{-1}$. Samples showing scattered NRM directions and higher intensity values of 270–555 $A.m^{-1}$ (*e.g.* GH07A, B) were discarded, most probably due to lightning effects.

An extremely stable magnetic component was reached for the NNW-trending Manso dolerite dykes after removing a secondary/viscous component. Linear behavior is generally observed with two well-defined segments in the Zijderveld plots with a "high coercivity/temperature component" revealed above AF values of 17 mT (**Fig. 3**A, E, and F) and temperature values range of ~540–580°C (**Fig. 3**B, C, and D). These unblocking temperatures (T_{ub}) point toward magnetite as the main carrier of the high-temperature component. Calculated by PCA analysis, a characteristic remanent magnetization (ChRM) is revealed for a first cluster (A+) of five sites showing a northern direction with a positive inclination (**Fig. 3**A, B). A second

cluster (A-) is composed of eight sites with a ChRM of southern direction with a steep negative inclination (**Fig. 3**C, D, and E).

A total of 165 specimens (13 sites) was used to calculate the Manso pole using the high coercivity-temperature component (**Fig. 4**A). Using the sites with positive inclinations (D_m = 16.6°, I_m = 76.7°, n = 5, k = 21) and the sites with negative inclinations (D_m = 172.8°, I_m = -77°, n = 8, k = 37.1), the Manso dyke swarm passes a reversal test with a critical gamma of 16.2° and a difference of 5.4° between normal and reverse axes (reversal test of C-class) (McFadden and McElhinny, 1990). 163 specimens show a secondary component with low inclination (**Fig. 4**B), and the subsequent secondary site-mean direction is D_m = 345.5°, I_m = -1.4° (α95 = 21.1°, k = 4.8) (**Fig. 4**C). The Manso pole (13 sites) was calculated using the 5 sites of positive inclinations and the 8 sites of negative inclinations (**Fig. 4**C) giving a site mean direction of D_m = 181.9°, I_m = -77.2° (α95 = 7.6°, k = 30.6), yielding to a paleomagnetic pole located at 28.3°S and 177.6°E (A95 = 12.7° K =11.6) (**Table 1**; **Fig. 4**C, D)

An iterative cutoff of 37.6° was determined using the 13 sites with no site exclusion (Vandamme, 1994), yielding a VGP dispersion (S-value) of 23.8° (**Fig. 4**D). High dispersion is expected for results with high inclination values as suggested by paleosecular models of latitudinal dependence of S (*e.g.* Model-G from McFadden et al. (1988)). The A95 for the Manso pole is equal to 12.7° which is comprised within the A95 envelope (4.3°–16.3°) of Deenen et al. (2011) (see **Fig. 4**D). Altogether, these characteristics suggest that our sampling of the Manso dolerite dykes average the paleosecular variation.

Though based on a single site (GH07), a stable ChRM of steep negative inclination and southwestern direction was obtained for the ~915 Ma E-trending Oda dyke, similar to the A-cluster of the Manso dykes (**Fig. 3**F) providing a VGP at 21°S and 222.3°E.

FIGURE 3

FIGURE 4

TABLE 1

4.3. Baked contact test

Due to the weathering cover, host rocks could only be sampled in the Ahafo mining pit (Newmont Company) in the Sefwi Belt (**Fig. 5**), to attempt a baked contact test (BCT). **Fig. 5**A shows the sampled outcrop where two undeformed lamprophyre dykes (GH11 as illustrated in **Fig. 5**B, and GH12) are cutting the granodiorite host rock deformed during the ~2000 Ma Eburnean orogeny (Feybesse et al., 2006). Two oriented blocks (OB3 and OB4) were collected for the GH12 dyke (**Fig. 5**A). To attest the primary origin of the magnetization carried by the dyke GH12, we sampled one oriented block (OB6) within the baked zone into a two- branched dyke. The oriented blocks OB7 and OB8 were sampled at ~1 m and ~30 m respectively from the GH12 dyke. Thermal demagnetizations revealed a high unblocking temperature interval (T_{ub}) of 520–620°C and high stability for the ChRM of the baked host rock at the contact (OB6) with a site-mean of D_m = 117.9° and I_m = 80.3° ($\alpha95$ = 4.9°, k = 112.8) (**Table 1**; **Fig. 5**C, D). The host rock at the contact shows the same ChRM direction of the GH12 dyke (D_m = 87.9° I_m = 86.8°, $\alpha95$ = 4°, k = 100.2) (**Table 1**; **Fig. 5**C, D). The secondary components are close to the present field with a northwestern direction and a low inclination for the dyke and the host rock. At ~1 m from the dyke, the OB7 block shows a significantly different behavior where thermal and AF demagnetizations reveal a more unstable magnetization (**Fig. 5**C), nevertheless magnetic vectors were defined for this block with two specimens providing a direction close to the dyke's direction and two specimens showing a western direction with low positive inclination (**Fig. 5**C). This western direction was also disclosed for the oriented block collected at ~30 m from the contact (OB8). Differently from the OB7 block, specimens from the OB8

block are well-clustered (D_m = 291.3° I_m = 31°, α95 = 7.6°, k = 46.7) with a stable ChRM until ~500°C. This baked contact test can be considered as positive and attests to the primary origin of the extremely stable ChRM disclosed in the Manso dykes.

FIGURE 5

4.4. Magnetic mineralogy

Most opaque phases show composite texture of ilmenite-magnetite and probably titanomagnetite (Haggerty, 1991). **Fig. 6**A shows a representative magnetite with ilmenite lamellae in a coarse-grained dolerite dyke (GH16). Intergrowth textures with ilmenite exsolutions are generally related to a stable thermoremanent magnetization (TRM) which supports our interpretation of the paleomagnetic results (Evans and Wayman, 1974). **Fig. 6**B shows three thermomagnetic curves, two for the Manso (GH08 and GH14) and one for the Oda dyke (GH07). The sample GH08A shows a curve with a reversible behavior between the heating and cooling steps whereas the cooling curve for samples GH14B3 and GH07B3 are not perfectly reversible. All samples show a Curie temperature (T_c) at about 560–580°C, and a Hopkinson peak for GH08 and GH14 just below T_c (Dunlop, 1974), characteristic of fine-grained pure magnetite. The Day plot (**Fig. 6**C) and FORC diagrams (**Fig. 6**D) indicate domain states mainly in the stable single-domain (SD) to pseudo-single domain (PSD) fields. Values of Mrs/Ms higher than 0.10, and the strong proportion of 60–40 % of single domains magnetite in the Day plot are consistent with the narrow unblocking temperatures above 540°C. FORC diagram of sample GH08H1 is typical of the PSD behavior (Roberts et al., 2014), with SD-like magnetite dominance of the magnetic assemblage as shown by the peak value of ~25 mT with closed contours on the H_u = 0 axis (**Fig. 6**D). Conversely, the GH03M1 sample show a strong proportion of multi-domain (MD) grains mixed with SD grains as suggested by a large coercivity distribution on the H_u axis. This SD/MD behavior is also confirmed by the position

of GH03M1 in the Dunlop (2002) mixing curves of the Day plot (**Fig. 6**D). GH15 sample fall in the MD field of the Day diagram which suggests a strong proportion of MD-like magnetite in the magnetic assemblage, consistent with the strong decay of ~50% of its NRM at 10 mT during AF pre-treatment (**Fig. 3**B). The host rocks fall into the PSD domain for samples at the contact, whereas samples far from the contact fall into the MD field of the Day plot (**Fig. 6**C), suggesting a less stable behavior for these rocks. This further confirms that the host rock at the contact was mineralogically affected and re-heated during the dyke's intrusion.

FIGURE 6

5. DISCUSSION

1.1. Reliability of the Manso paleomagnetic pole (R-criteria)

The Manso paleomagnetic pole was calculated with 13 sites of NNW- trending mafic dykes in Ghana and satisfies all seven criteria of the revised **"R"** reliability index (Meert et al., 2020). (**R1**) The Manso dyke swarm is well-dated by multi-method radiometric dating with one U-Pb baddeleyite (ID-TIMS) age of 867 ± 16 Ma ($^{207}Pb/^{206}Pb$ weighted mean age) (GH08) (Baratoux et al., 2019) and two identical (within error) U-Pb apatite ages of 857.2±8.5 Ma (GH05) and 855 ± 16 Ma (GH16) (**Fig. 2**). Given that the U-Pb apatite system (Chew and Spikings, 2015) has a lower closure temperature (550–350°C) than the U-Pb baddeleyite system (700–1100°C) (Heaman and LeCheminant, 2001), these identical ages within error suggest the U-Pb apatite system recorded the age of crystallization. Using the U-Pb baddeleyite $^{207}Pb/^{206}Pb$ weighted mean age of 867 ± 16 Ma (*or the Concordia age: 855 ± 10 Ma*) (Baratoux et al., 2019) combined with the two new U-Pb apatite ages, a mean age of 858.6 ± 6.7 (*856.1 ± 6*) Ma can be calculated for the emplacement of the NNW-trending Manso dyke swarm. (**R2**) ChRM directions were isolated on 13 sites (165 specimens) by thermal and AF demagnetizations and no difference was observed between the two demagnetization methods. Moreover, all vectors were well-defined by stable linear segments reaching the origin (**Fig. 3**), and analyzed by PCA analysis

using Zijderveld plots and equal-area projections (Kirschvink, 1978; Zijderveld, 1967). Our new Manso pole is characterized by a value of precision K of 11.6, above the lower limit of 10 proposed by (Meert et al., 2020). In addition, the A95 of 12.7° is comprised within the Deenen et al. (2011)'s interval (4.3°–16.3°) showing that the pole averages the paleosecular variation (**Fig. 4**D). No VGPs were excluded by the iterative cutoff of Vandamme (1994). (**R3**) The magnetic properties of these mafic dykes confirm their remanent magnetization is carried by a magnetic assemblage dominated by SD-like magnetite (**Fig. 6**). (**R4**) A positive baked contact test for the GH12 dyke confirms the remanence is primary. In addition, a primary origin is also suggested by the narrow and high unblocking temperatures (T_{ub}) (540–580°C) of the Manso dykes which are above those of the undisturbed U-Pb apatite system (550-350°C). (**R5**) These undeformed dykes were sampled in a vast geographic area in Ghana considered as stable and without evidence of deformation related to the Pan-African belts or younger tectonic events. Moreover, geochronological and paleomagnetic results of distant sites (*e.g.* between GH05 and GH16, which are 233 km apart from each other) support a strong regional consistency in our results. The younger events in the area were associated with the magmatic activity of the Central Atlantic Magmatic Province (CAMP) and the Atlantic rifting between Africa and South America (Baratoux et al., 2019). These events produced a low-temperature regional influence of <120°C (Fernie et al., 2018), not sufficient to affect the primary magnetization of the dykes. This is consistent with the secondary component calculated for most of dykes with a corresponding pole located at 73.1°N, 244.8°E (**Table 1**), similar to the CAMP pole of 73°N, 244.7°E obtained for West Africa (Palencia-Ortas et al., 2011) (**Fig. 4**B). (**R6**) The Manso pole passes a reversal test (McFadden and McElhinny, 1990) with 5 sites of positive inclination and 8 sites of negative inclination. (**R7**) The A95 envelope of Manso pole overlaps the robust B2 group (R = 6) of Robert et al. (2017) for volcanic units of ~550–530 Ma sampled in the Anti-Atlas mountains, north of the West African Craton. Nevertheless, Meert et al. (2020) underline

that comparison to younger poles should be discarded if the younger poles come from an orogenic belt, which is the case with the B2 pole, calculated from units folded during the Carboniferous–Permian Hercynian (or Variscan) orogeny (Robert et al., 2017). Therefore, a remagnetization of the Manso dykes seems improbable because no evidence of deformation has been documented in the study area, and our large spatial sampling discard any localized tectonic rotations. Thus, we can consider that the Manso pole fulfills all the R7 criteria of Meert et al. (2020). The ~860 Ma Manso paleomagnetic pole can thus be considered as a high-quality key pole and can serve as the first Neoproterozoic reference for the paleogeography of West Africa during Rodinia.

1.2. Testing the existence of the long-lived WABAMGO configuration in Rodinia

The Grenville, Sveconorwegian, and Sunsás orogens are typically used to reflect the collision between Laurentia, Baltica and Amazonia between ~1200 and 1000 Ma assembling the Rodinia supercontinent (Hoffman, 1991). This combination between these cratons is nearly identical in several Rodinia reconstructions but was questioned by Meert and Torsvik (2003), and more recently by Evans (2009) using an updated paleomagnetic database. Recently, Martin et al. (2020) re-evaluated the isotopic signature of the long-lived Paleo– to Mesoproterozoic accretionary orogens along the margins of Laurentia, Baltica, Amazonia, and Kalahari**.** In their model, the core of Rodinia is defined by the Laurentia-Baltica-Amazonia-Kalahari connection finally sutured during the Stenian. In the Rodinian reconstructions, West Africa is still associated with the Amazonia Craton but without paleomagnetic constrains (D'Agrella-Filho et al., 2016), we can use our new paleomagnetic results to test if a long-lasting connection is paleomagnetically viable between Amazonia, West Africa and the paleomagnetically well-constrained Baltica and Laurentia block.

A long-lived connection is usually proposed for Baltica and Laurentia between ~1760 Ma and ~1270 Ma (Salminen et al., 2014). A large distance is observed across the APW path of

Baltica between the mean 1265 Ma pole (BA1) (Pesonen et al., 2003), the Salla diabase VGP (BA2) and the 1100-1050 Ma poles (BA3, BA4) (**Table 2**; **Fig. 7**A) (Mertanen et al., 1996; Pesonen et al., 2003) and suggests fast drifting at that time. A similar trajectory is observed for Laurentia with the Logan loop and the ~1105-1080 Ma Keweenawan track (LA1-LA2) (Swanson-Hysell et al., 2019). Between ~1050 and 900 Ma the APW path of Laurentia was defined as the Grenville loop and the same interval in Baltica was defined as the Sveconorwegian loop, but its shape and motion are debated (Elming et al., 2014; Gong et al., 2018). The best attempts to adjust the Grenville and Sveconorwegian loops are along an Euler pole of 75.8°N, 264.2°E, -59.2° (Pisarevsky et al., 2003), or in a tighter fit of 81.5°N, 250°E, -50° (Evans, 2009). However, Baltica rotated ~70° clockwise in relation to Laurentia between the ~1800–1200 Ma NENA (Northern Europe-North America) configuration (Gower et al., 1990) and the ~1050–800 Ma Rodinia configuration (Salminen et al., 2009). If these reconstructions hold true, they imply a single Laurentia-Baltica block between ~1050 and 800 Ma. Key 951-935 Ma mean poles for Baltica (BA6) confirmed this clockwise motion, but a more complex shape for the APW path is proposed considering the ~971 Ma VGP of Blekinge-Dalarma dykes (Group. B) (BA5) (**Fig. 7**A) (Gong et al., 2018). A late Svecornorwegian group of poles (936–850 Ma) obtained for the Rogaland Igneous Complex (RIC) and the ~860 Ma Hunnedalen dykes with a stable remanence of same polarity suggest a stable position for Baltica at high latitude (BA7-BA11) (Walderhaug et al., 1999). The primary remanence of this group is supported by an inverse contact test with the ~635 Ma Egersund dyke swarm (Walderhaug et al., 2007).

West Africa is always associated with the Amazonia Craton in the Paleo-Mesoproterozoic reconstructions but in a different position from the Gondwana link (Onstott and Hargraves, 1981). These cratons were juxtaposed with the Baltica in the **S**outh **Am**erica **Ba**ltica (**SAMBA**) connection with the possibility of a long-lived connection between ~1800 and 800 Ma

(Johansson, 2009). An alternative reconstruction, using geological considerations, was proposed with Kalahari-Congo, São Francisco and India in the Umkondia supercraton at ~1110 Ma (Choudhary et al., 2019). Using the paleomagnetic poles of the ~1199 Ma Nova Floresta formation (AM1) (D'Agrella-Filho et al., 2008) and ~1149 Ma Fortuna formation (AM2) (Tohver et al., 2002) (**Fig. 7**A), a strike-slip migration of Amazonia along the Laurentia at ~1200–1150 Ma was initially proposed. But, a preliminary ~1110 Ma paleomagnetic pole for the well-dated Rincon del Tigre Complex (AM3) (Teixeira et al., 2015) supports a moderate to low latitude for Amazonia at that time (Patroni, 2015), which is incompatible with the model of oblique collision proposed by Tohver et al. (2002). These AM3 pole for Amazonia supports the model of Evans (2013) suggesting a clockwise rotation of the Amazonia and Baltica to collide with Laurentia. For West Africa, paleomagnetic results were obtained from the Mesoproterozoic units of the Adrar (NW- West Africa, Mauritania) (Morris and Carmichael, 1978; Perrin et al., 1988; Perrin and Prévot, 1988). Rooney et al. (2010) obtained a new Re-Os age of ~1105 Ma for the Atar group previously estimated at 890–775 Ma. Based on the similarity with younger directions some authors have suggested some remagnetization effects (Perrin and Prévot, 1988; Tohver et al., 2006), but without further evidence that the primary origin for their remanence cannot be ruled out. The characteristic component for those rocks is carried by hematite and was revealed at high temperatures (>590°C). If the magnetization is primary this allows to define a new Mesoproterozoic age of ~1105 Ma for the I9 pole (WA1) calculated by Perrin and Prévot (1988) coeval to the ~1110 Ma Rincon del Tigre pole (AM3) from the Amazonia Craton (Patroni, 2015) (**Fig .7**A). No data are available to define the APW path for the Amazonia Craton in Early Neoproterozoic times, but our new ~860 Ma Manso pole satisfies a maximum R-criteria to be considered as an anchor point for paleogeographic reconstructions (**Fig.7**A; R = 7, **this study**).

The Mesoproterozoic APW path for the Congo-São Francisco Craton is defined by the well-dated Late Kibaran pole (C1) at ~1236 Ma (Meert et al., 1994b). A large shift is observed between the ~1110 Ma pole from the Huile-Epembe dykes (Salminen et al., 2018) and the ~925 Ma poles from the São Francisco dykes (Salvador, Ilhéus, Oliveira) (**Fig. 7**A) D'Agrella-Filho et al. (1990); (D'Agrella-Filho et al., 2004; Evans et al., 2016). The Congo-São Francisco Craton is usually associated with the Rodinia supercontinent (Merdith et al., 2017), or in a different view connected with the African blocks (D'Agrella-Filho and Cordani, 2017).

Similarities in length and shape of the APW paths for Baltica, Amazonia, West Africa, and São Francisco-Congo cratons allow us to build a Master APW path between ~1200 and 850 Ma for these continental units (**Fig. 7**A). This Master APW path suggests that these blocks were nearby between ~1200 and 850 Ma, forming a single continental entity. This large continental unit, hereafter referred to **WABAMGO** (**W**est **A**frica-**B**altica-**Am**azonia-Con**go**) is represented in **Fig. 7**B. Geological domains, LIPs comparisons, and paleomagnetic data between Baltica, Amazonia, and West Africa support a strong connection between these continents since the Paleoproterozoic using the SAMBA model (Baratoux et al., 2019; D'Agrella-Filho et al., 2016; Terentiev and Santosh, 2020). Our model supports the presence of a long-lived accretionary margin during the Mesoproterozoic times in the western part of Amazonia (Sadowski and Bettencourt, 1996). The orientation of West Africa in relation to Amazonia in the SAMBA model is paleomagnetically viable from ~2100 Ma until ~1400 Ma (D'Agrella-Filho et al., 2016), but a later reorientation is necessary to fit with the classical ~550 Ma Gondwana configuration. In the WABAMGO configuration, the West Africa-Amazonia connection is close to this late Neoproterozoic configuration, suggesting this reorientation could have occurred between ~1400 and 1200 Ma, during the breakup of the Columbia supercontinent. The Sunsás and Sveconorwegian orogens can be correlated between Amazonia and Baltica in this model (**Fig. 7**B). A large Early Tonian mafic magmatism is observed in the São Francisco

craton spanning from ~925 Ma to 850 Ma (Danderfer et al., 2009; Moreira et al., 2020). Similar records of Tonian age magmatism have been reported for the Congo with the Sembé Ouesso (Vicat and Pouclet, 1995), for Baltica with the ~850 Ma Hunnedalen dykes (Walderhaug et al., 1999), for Amazonia with the ~809 Ma Makinet (ex-Tampok) dykes ((Delor et al., 2003), and also for West Africa with the ~860 Manso and ~915 Oda dykes in the south of the craton (Baratoux et al., 2019) and the ~880-850 Iguerda-Taïfast dykes in the Anti-Atlas (Kouyaté et al., 2013). An Early Tonian rifting is also documented for the northern part of the West African Craton with the volcanoclastic deposits of the ~883 Ma Tachdamt Fm (Bouougri et al., 2020). An Early Tonian rifting between the northern West Africa and the São Francisco is thus supported by the WABAMGO configuration (**Fig. 7**B). A rare "Grenvillian event" (~1000–920 Ma) documented within the WABAMGO juxtaposition is the Cariris Velhos tectonic event, proving some continental reorganization and convergence at the edge of the mega block of the Borborema Province was followed by a Tonian rifting (dos Santos et al., 2010; Neves et al., 2020).

Our model also supports a "Grenvillian" source for zircons in northern West Africa (Bouougri et al., 2020; Kalsbeek et al., 2008) with the proximity of the Grenvillian orogens to the west such as Sunsás and Sveconorwegian and the associated small blocks (*e.g.* Oaxaquia, Maya), and the Cariri Velhos event to the east. Major shifts in the sedimentation on the West African Craton suggest a complete breakup of the WABAMGO from Baltica and São Francisco-Congo after ~800 Ma with the development of subduction zones in northern West Africa in the late Neoproterozoic (Triantafyllou et al., 2016). Following this model, the proximity of the Congo-São Francisco and West Africa may explain the large displacements along the major dextral Transbrasiliano lineament with the closure of the Pharusian Ocean during the assembly of Gondwana in late Neoproterozoic times. The proposed long-lived

WABAMGO juxtaposition is geologically and paleomagnetically viable between ~1200 and 800 Ma.

1.3. Implications for the Rodinia assembly

Using our new Master APW path for the West Africa-Baltica-Amazonia-Congo block, the reconstruction at ~1110 Ma shows that the assembly of Rodinia is dominated by the V-shape closure of the external Nuna Ocean (Li et al., 2019), or Grenville Ocean, (Sadowski and Bettencourt, 1996), between the northern Laurentian blocks and the southern WABAMGO (**Fig. 8**A). This hypothesis of the closure of this Ocean by accretionary orogens was previously suggested on geological grounds (Cawood and Pisarevsky, 2017; Martin et al., 2020), but our study add a paleomagnetic support. The Kalahari craton is positioned in **Fig. 8** along the southern tip of Congo (pos-A) as in (Salminen et al., 2018) or in its inverted position (pos-B) with the Natal-Namaqua orogen facing the coeval Grenville orogen in Laurentia, in both cases constrained by the ~1109 Ma Umkondo pole (K1) (Swanson-Hysell et al., 2015a). In the preferred position B, the Kalahari craton will collide with the southern coast of Laurentia after the closure of the external Nuna Ocean (**Fig. 8**B). Nevertheless, the Kalahari position is poorly constrained in Rodinia, and is beyond the scope of this contribution. The orientation of West Africa in the WABAMGO configuration (pos-A, **Fig. 8**B) differs from the SAMBA model, in which the western margin of West Africa is associated to the southern part of Baltica. Nevertheless, our new proposed configuration requires new Tonian high-quality poles for the unconstrained cratons, especially Amazonia, and new Mesoproterozoic poles for West Africa to confirm the relative orientation between Amazonia and West Africa. Discarding the ~1105 Ma WA1 pole, a position closer to the SAMBA model (Johansson, 2009) is paleomagnetically plausible for West Africa (pos-B, **Fig. 8**B).

For the final paleogeographic configuration at 925-850 Ma we can compare the position of West Africa derived from the Manso paleomagnetic pole with the available record of Laurentia

and surrounding blocks (**Fig. 8**C). Three paleomagnetic poles are available for the northern blocks of Rodinia. Laurentia can be constrained by the basal units from the Little Dal Group, LA3 pole, which passes a fold test, and its age was recently constrained by high-quality correlations between 892 and 849 Ma (Greenman et al., 2020; van Acken et al., 2013). One pole for the Tarim (T1) at ~880 Ma (Wen et al., 2018), and one pole for North China at ~895 Ma (NC1) (Fu et al., 2015) complete the paleomagnetic database for the northern blocks of Rodinia. Our model implies that Rodinia was formed by extroversion (Murphy and Nance, 2003), with the closure of an external Nuna Ocean between two large blocks, the southern WABAMGO and the northern Laurentian block. Rodinia was finally assembled by a large dextral motion of the Australia-Tarim blocks as suggested by Wen et al. (2018). The polar location of the WABAMGO at ~900 Ma, together with the low-mid latitudinal distribution of Laurentia and the blocks of North China, Tarim, Australia (?) confirms a pan-latitudinal rather than an equatorially distributed supercontinent as suggested by Jing et al. (2019).

FIGURE 7

FIGURE 8

TABLE 2

6. CONCLUSIONS

New U-Pb apatite ages of 857.2±8.5 Ma and 855±16 Ma agree with the previous 867±16 Ma U-Pb baddeleyite age (Baratoux et al., 2019) confirming the extension of the Manso dyke swarm to the north of Ghana. A ~860 Ma Manso key pole (28.3°S, 177.6°E, A95 = 12.7°, R = 7) was calculated and represent the first high-quality paleomagnetic data in Early Tonian for the West African craton. The remagnetization is considered as primary, passing a baked contact test and a reversal test. The paleomagnetic database for West Africa, Baltica, Amazonia, and the Congo-São Francisco cratons supports a long-lived continental unit between ~1200 and 800

Ma, the WABAMGO juxtaposition. During the late Mesoproterozoic-Early Neoproterozoic (~1200–900 Ma), the WABAMGO and the Laurentia were drifting southward. During this migration, a clockwise rotation of the WABAMGO in relation to Laurentia closed the external Nuna Ocean causing the Grenvillian collisions suturing the Rodinia supercontinent. Thus, this model favors with paleomagnetic support the formation of the Rodinia supercontinent by extroversion.

ACKNOWLEDGEMENTS

We thank the Brazilian Fundação de Amparo à Pesquisa do Estado de São Paulo (FAPESP grants 2017/18840-6, 2018/23755-0) for financial support of the postdoctoral fellowship (Paul Yves Jean Antonio), and funding of the associated thematic project of Ricardo Ivan Ferreira Trindade (2016/06114-6). We thank the Geological Survey of Authority of Ghana, especially Mahu Eric Nene for field-trip logistics. We thank the Newmont Company, Ltd. of Ahafo mine and the regional director Paul Morley, for accommodation, accessibility to the site and facilities. We thank Philippe de Parseval and Loic Drigo for help during analytical work in Toulouse, and Pierre Camps for access to his duty standing drill press (Géosciences Montpellier). We thank the infrastructure of “Centro Oceanográfico de Registros Estratigraficos (CORE), Instituto Oceanográfico da Universidade de São Pauo” for using the VSM. Thanks to Helen McFarlane, Stephane Perrouty and Quentin Masurel for the sampling location preparation. This work would not have been possible without the assistance and hospitality of Ghanaian communities (Amanfro, Domeabra, …).

FIGURE AND TABLE CAPTIONS

Fig. 1: Inset: Location of the study area in the West African craton (WAC). Geological map of the Neoproterozoic units of Ghana with sampling location for geochronology (red stars) and paleomagnetism. *: U-Pb baddeleyite age of GH08 = 867 ± 16 Ma (Manso) and GH07 = 915 ± 7 Ma (Oda) from Baratoux et al. (2019). **: U-Pb apatite ages of GH05 = 857.2 ± 8.5 Ma and GH16 = 855 ± 16 Ma from **this study**.

Fig. 2: **A** and **B:** Field photographs of the Manso dolerite dykes at GH05 and GH16 sites, respectively. **C** and **D:** U-Pb Terra-Wasserburg diagrams for apatite dating of the Manso dolerite dykes at GH05 (C) and GH16 (D) sites. The upper intercept is anchored to the initial Pb Pb ratio (0.898) that was calculated based on Pb model of Stacey and Kramers (1975) for an emplacement age of ~867 Ma (Baratoux et al., 2019). Unanchored ages are also illustrated (in red).

Fig. 3: Representative demagnetization plots of Neoproterozoic dykes for different geographic sites in Ghana after AF and thermal demagnetizations. Equal-area stereonets (filled (open) symbols represent positive inclination), Zijderveld plots (vertical/horizontal projections shown by open/filled circles), and Magnetization intensity decay curves (M/Mmax) are indicated for each example. Values of 75% of the NRM decay (in mT) and unblocking temperature spectra are indicated for the AF and thermal demagnetization curves, respectively. NRM = natural remanent magnetization. Numbers, T100 (A5), indicate thermal (AF) demagnetization step.

Fig. 4: Sample and site mean directions for the Manso dykes. **A:** Specimen mean directions of the high coercivity/temperature components (in green). **B:** Specimen mean directions of the low coercivity/temperature components (in purple). **C:** Site mean directions for the Manso dykes (in green), the secondary site mean directions is also indicated (in purple). Sites/specimens with positive and negative inclinations are represented with filled (open) symbols represent

downward (upward) inclinations. Confidence circle (α95) around the means are indicated. PDF – Present dipolar geomagnetic field; PGF – Present geomagnetic field. **D:** Dispersion of site mean virtual geomagnetic poles (VGPs) and paleomagnetic pole calculated for the Manso dykes (**Table 1**) represented in a Schmidt projection. Deenen et al. (2011)'s A95 envelope (4.3°–16.3°) and the iterative cutoff limit (37.6°) of Vandamme (1994) are indicated. *: U-Pb baddeleyite age of GH08 = 867 ± 16 Ma (Manso) and GH07 = 915 ± 7 Ma (Oda) from Baratoux et al. (2019). **: U-Pb apatite ages of GH05 = 857.2 ± 8.5 Ma and GH16 = 855 ± 16 Ma from this study. Direction and VGP for the ~915 Ma site (GH07) are indicated in grey, not considered for the Manso pole.

Fig. 5: Baked contact test for the GH12 dyke (~1 m in width). **A:** Geological sketch of the outcrop with location of the sampled oriented blocks (star) of dykes (in green), and the host rocks at contact (in red), at ~1m (in pink), and at ~30m (in blue) from the contact. **B:** Field photograph of the GH11 lamprophyre dyke, 0.30 m wide, located in (**A**). **C:** Equal-area stereonets (filled (open) symbols represent positive inclination) of site-mean directions for the GH12 dyke (in green) and the subsequent host rocks at contact (in red), at ~1m (in pink), and ~30m (in blue) from the contact. Magnetization intensity decay curves (M/Mmax) are indicated. **D:** Zijderveld plots for representative specimens after thermal demagnetization from the GH12 dyke (OB4A1), the host rock at contact (OB6A2b) and at ~30m (OB8E1).

Fig. 6: A: SEM-BSE micrograph of titanomagnetite (Mag) with exsolutions of ilmenite (Ilm), augite (Aug), plagioclase (Pl), spharelite (Sp), and apatite (Ap) for the GH16 dyke. **B:** Heating (in red) and cooling (in blue) thermomagnetic curves for three samples (GH14B3, GH07B3, and GH08A). **C:** Day plot for the Manso dykes and the host rocks with SP-MD mixture lines indicating the single domain proportions. SD: single domain, PSD (or vortex state): pseudo-single domain, MD: multidomain. **D:** First-order reversal curve (FORC) diagrams for the

GH08H1 and the GH03M1 specimens. SF is the smoothing factor used by the FORCOT software.

Fig. 7: A: The **WABAMGO** (**W**est **A**frica-**B**altica-**Am**azonia-Con**go**) juxtaposition using Baltica as reference frame in present coordinates. Euler poles used in the Baltica reference frame for the different cratons in the WABAMGO configuration: West Africa (1.375°N, 15.1585°E, -66.0819°), Amazonia (10.894°S, 369.8179°E, -89.4471°), Congo (52.32°S, 158.71°E, -70.57°). The São Francisco craton is rotated to Congo using its pre-Mesozoic configuration (46.8°N, 329.4°E, 55°, (McElhinny et al., 2003)). Kalahari is connected to the Congo craton (12.8°S, 19°E, -43.2°) according the configuration of Salminen et al. (2018). Present North is indicated for each craton by an arrow. ***Abbreviations for the ~1200–1000 Ma Grenvillian orogens (in black):*** (1) Sveconorwegian orogen, (2) Sunsás orogen, (3) Cariris Velhos event, (4) Namaqua-Natal orogen. Tonian large igneous provinces (LIPs, in red) are indicated. **B:** Master apparent polar wander (APW) path for the WABAMGO between ~1200 and 850 Ma. Paleomagnetic poles and used abbreviations are listed in the **Table 2**.

Fig. 8: A: Paleogeography reconstruction of the Rodinia assembly at ~1110 Ma showing the presence of the external Nuna Ocean (Grenville Ocean) between the WABAMGO (south Rodinia) and the Laurentia (north Rodinia). Two plausible positions are illustrated for the Kalahari craton with the Salminen et al. (2018) configuration (pos-A), and Kalahari placed in the west of Amazonia (pos-B) as paleolongitude is arbitrary. We followed the model of Sadowski and Bettencourt (1996) using a subduction towards Amazonia. **B:** Paleogeography reconstruction of the Rodinia at ~925–850 Ma. Cratons with paleomagnetic constraints (in colors) and cratons with no data (?) are indicated. Two positions of West Africa are illustrated with the position A in agreement with the WABAMGO configuration and the plausible position B according the uncertainty for the paleolongitude. The hypothesis of a dextral movements from Wen et al. (2018) is indicated for the northern cratons of Australia-Mawson-Tarim. **C:**

Paleomagnetic poles (north pole) used in the reconstruction at ~925–850 Ma (**B**). See **Table 2** for abbreviations and references.

Table 1: S.lat, S.lon are the site latitude and longitude. n/N - number of specimens used in mean directions/number of analyzed specimens; Dec – Declination; Inc – Inclination; R – the resultant vector, α95 (*A95*) is the radius of the 95% cone of confidence and k (*K*) is the precision parameter - Fisher's statistical parameters (Fisher, 1953) for the mean directions (*mean virtual geomagnetic poles – VGPs*); P.Lat – pole latitude; P.Long – pole longitude. Values of mean sites directions are indicated in bold for the positive, negative, and combined polarities. *: U-Pb baddeleyite age of GH08 = 867 ± 16 Ma (Manso) and GH07 = 915 ± 7 Ma (Oda) from Baratoux et al. (2019). **: U-Pb apatite ages of GH05 = 857.2 ± 8.5 Ma and GH16 = 855 ± 16 Ma from this study. ¥: Site with an attempted baked contact test (BCT). γ (γc = critical) is the angle calculated between the mean directions of reversed and normal polarities (McFadden and McElhinny, 1990).

Table 2: Paleomagnetic database for the Rodinia. Code, Plat – pole latitude, Plon – Pole longitude, Age – nominal age, A95 confidence cones of the paleomagnetic poles used in the paleogeographical reconstructions. R-criteria from Meert et al. (2020). ***References:*** **Laurentia**: [1] Park (1981), [2] Swanson-Hysell et al. (2019), **Baltica:** [3] Walderhaug et al. (1999), [4] Brown and McEnroe (2004), [5] Stearn and Piper (1984), [6] Walderhaug et al. (2007), [7] Brown and McEnroe (2015), [8] Gong et al. (2018), [9] Mertanen et al. (1996), [10] Pesonen et al. (2003), [11] Salminen et al. (2009), **West Africa:** [12] **This study**, [13] Perrin and Prévot (1988), [14] Rooney et al. (2010), **Amazonia:** [15] Patroni (2015), [16] Teixeira et al. (2015) [17] D'Agrella-Filho et al. (2008), [18] Tohver et al. (2002), **Congo-São Francisco:** [19] Evans

et al. (2016), [20] D'Agrella-Filho et al. (2004), [21] D'Agrella-Filho et al. (1990), [22] Salminen et al. (2018), [23] Meert et al. (1994a), **Kalahari:** [24] Swanson-Hysell et al. (2015a), **North China:** [25] Fu et al. (2015), **Tarim:** [26] Wen et al. (2018).

S1: Apatite U-Pb isotope data.

S2: Analytical conditions for apatite LA-ICP-MS dating.

REFERENCES

Affaton, P., Rahaman, M.A., Trompette, R., Sougy, J., 1991. The Dahomeyide Orogen: Tectonothermal Evolution and Relationships with the Volta Basin, In: Dallmeyer, R.D., Lécorché, J.P. (Eds.), The West African Orogens and Circum-Atlantic Correlatives. Springer Berlin Heidelberg, Berlin, Heidelberg, pp. 107-122.

Antonio, P.Y., Baratoux, L., Da Trindade, R.I., Rousse, S., Macouin, M., Firmin, A.-S., Martinez-Dopico, C.I., Anani, A.P.A., WK, A.E., Amponsah, P.O., 2019. PRELIMINARY IN PHASE AND OUT OF PHASE AMS STUDY AND PALEOMAGNETISM OF~ 870 MA MAFIC DIKES IN WEST AFRICA (GHANA), In: Letters, L. (Ed.), 2019 Biennial Meeting of Latinmag, Proceedings Rancagua, Chile, pp. B18-P, 11-17.

Baratoux, L., Söderlund, U., Ernst, R., de Roever, E., Jessell, M., Kamo, S., Naba, S., Perrouty, S., Metelka, V., Yatte, D., 2019. New U–Pb Baddeleyite Ages of Mafic Dyke Swarms of the West African and Amazonian Cratons: Implication for Their Configuration in Supercontinents Through Time, Dyke Swarms of the World: A Modern Perspective. Springer, pp. 263-314.

Berndt, T.A., Chang, L., 2019. Waiting for Forcot: Accelerating FORC Processing 100× Using a Fast-Fourier-Transform Algorithm. Geochemistry, Geophysics, Geosystems 20, 6223-6233.

Black, R., Caby, R., Moussine-Pouchkine, A., Bayer, R., Bertrand, J., Boullier, A., Fabre, J., Lesquer, A., 1979. Evidence for late Precambrian plate tectonics in West Africa. Nature 278, 223.

Bond, G.C., Nickeson, P.A., Kominz, M.A., 1984. Breakup of a supercontinent between 625 Ma and 555 Ma: new evidence and implications for continental histories. Earth and Planetary Science Letters 70, 325-345.

Bonhomme, M., 1962. Contribution à l'étude géochronologique de la plateforme de l'Ouest africain. Géologie et Minéralogie, vol. 5. Thesis. University of Clermont-Ferrand, Fr.

Bouougri, E.H., Lahna, A.A., Tassinari, C.C.G., Basei, M.A.S., Youbi, N., Admou, H., Saquaque, A., Boumehdi, M.A., Maacha, L., 2020. Time constraints on Early Tonian Rifting and Cryogenian Arc terrane-continent convergence along the northern margin of the West African craton: Insights from SHRIMP and LA-ICP-MS zircon geochronology in the Pan-African Anti-Atlas belt (Morocco). Gondwana Research 85, 169-188.

Brown, L.L., McEnroe, S.A., 2004. Palaeomagnetism of the Egersund-Ogna anorthosite, Rogaland, Norway, and the position of Fennoscandia in the Late Proterozoic. Geophysical Journal International 158, 479-488.

Brown, L.L., McEnroe, S.A., 2015. 916 Ma Pole for southwestern Baltica: palaeomagnetism of the Bjerkreim-Sokndal layered intrusion, Rogaland Igneous Complex, southern Norway. Geophysical Journal International 203, 567-587.

Cawood, P.A., Pisarevsky, S.A., 2017. Laurentia-Baltica-Amazonia relations during Rodinia assembly. Precambrian Research 292, 386-397.

Chew, D.M., Sylvester, P.J., Tubrett, M.N., 2011. U–Pb and Th–Pb dating of apatite by LA-ICPMS. Chemical Geology 280, 200-216.

Chew, D.M., Spikings, R.A., 2015. Geochronology and Thermochronology Using Apatite: Time and Temperature, Lower Crust to Surface. Elements 11, 189-194.

Choudhary, B.R., Ernst, R.E., Xu, Y.G., Evans, D., de Kock, M., Meert, J., Ruiz, A., Lima, G.A., 2019. Geochemical characterization of a reconstructed 1110 Ma Large Igneous Province. Precambrian Research, 105382.

Cogné, J.P., 2003. PaleoMac: A Macintosh™ application for treating paleomagnetic data and making plate reconstructions. Geochemistry, Geophysics, Geosystems 4, 1007.

Condie, K.C., 2002. The supercontinent cycle: are there two patterns of cyclicity? Journal of African Earth Sciences 35, 179-183.

D'Agrella-Filho, M.S., Pacca, I.G., Renne, P.R., Onstott, T.C., Teixeira, W., 1990. Paleomagnetism of Middle Proterozoic (1.01 to 1.08 Ga) mafic dykes in southeastern Bahia State—São Francisco Craton, Brazil. Earth and Planetary Science Letters 101, 332-348.

D'Agrella-Filho, M.S., Tohver, E., Santos, J.O.S., Elming, S.-Å., Trindade, R.I.F., Pacca, I.I.G., Geraldes, M.C., 2008. Direct dating of paleomagnetic results from Precambrian sediments in the Amazon craton: Evidence for Grenvillian emplacement of exotic crust in SE Appalachians of North America. Earth and Planetary Science Letters 267, 188-199.

D'Agrella-Filho, M.S., Pacca, I.I.G., Trindade, R.I.F., Teixeira, W., Raposo, M.I.B., Onstott, T.C., 2004. Paleomagnetism and 40Ar/39Ar ages of mafic dikes from Salvador (Brazil): new constraints on the São Francisco craton APW path between 1080 and 1010 Ma. Precambrian Research 132, 55-77.

D'Agrella-Filho, M.S., Bispo-Santos, F., Trindade, R.I.F., Antonio, P.Y.J., 2016. Paleomagnetism of the Amazonian Craton and its role in paleocontinents. Brazilian Journal of Geology 46, 275-299.

D'Agrella-Filho, M.S., Cordani, U.G., 2017. The Paleomagnetic Record of the São Francisco-Congo Craton, In: Heilbron, M., Cordani, U.G., Alkmim, F.F. (Eds.), São Francisco Craton, Eastern Brazil: Tectonic Genealogy of a Miniature Continent. Springer International Publishing, Cham, pp. 305-320.

Dalziel, I.W.D., 1997. OVERVIEW: Neoproterozoic-Paleozoic geography and tectonics: Review, hypothesis, environmental speculation. Geological Society of America Bulletin 109, 16-42.

Danderfer, A., De Waele, B., Pedreira, A.J., Nalini, H.A., 2009. New geochronological constraints on the geological evolution of Espinhaço basin within the São Francisco Craton—Brazil. Precambrian Research 170, 116-128.

Deenen, M.H.L., Langereis, C.G., van Hinsbergen, D.J.J., Biggin, A.J., 2011. Geomagnetic secular variation and the statistics of palaeomagnetic directions. Geophysical Journal International 186, 509-520.

Delor, C., Lahondère, D., Egal, E., Lafon, J.M., Cocherie, A., Guerrot, C., Truffert, C., Théveniaut, H., Phillips, P., Avelar, G.V., 2003. Transamazonian crustal growth and reworking as revealed by the 1: 500,000-scale geological map of French Guiana (2nd ed.). Géologie de la France.

Donnadieu, Y., Godderis, Y., Ramstein, G., Nedelec, A., Meert, J., 2004. A /`snowball Earth/' climate triggered by continental break-up through changes in runoff. Nature 428, 303-306.

dos Santos, E.J., Schmus, W.R.V., Kozuch, M., Neves, B.B.d.B., 2010. The Cariris Velhos tectonic event in Northeast Brazil. Journal of South American Earth Sciences 29, 61-76.

Dunlop, D., 1974. Thermal enhancement of magnetic susceptibility. Journal of Geophysics| IF 32.18 40, 439-451.

Dunlop, D.J., 2002. Theory and application of the Day plot (Mrs/Ms versus Hcr/Hc). 1. Theoretical curves and tests using titanomagnetite data. Journal of geophysical research 107, EPM4.1-EPM4.22.

Elming, S.-Å., Pisarevsky, S.A., Layer, P., Bylund, G., 2014. A palaeomagnetic and 40Ar/39Ar study of mafic dykes in southern Sweden: A new Early Neoproterozoic key-pole for the

Baltic Shield and implications for Sveconorwegian and Grenville loops. Precambrian Research 244, 192-206.

Evans, D.A.D., 2009. The palaeomagnetically viable, long-lived and all-inclusive Rodinia supercontinent reconstruction. Geological Society, London, Special Publications 327, 371-404.

Evans, D.A.D., 2013. Reconstructing pre-Pangean supercontinents. Geological Society of America Bulletin 125, 1735-1751.

Evans, D.A.D., Trindade, R.I.F., Catelani, E.L., D'Agrella-Filho, M.S., Heaman, L.M., Oliveira, E.P., Söderlund, U., Ernst, R.E., Smirnov, A.V., Salminen, J.M., 2016. Return to Rodinia? Moderate to high palaeolatitude of the São Francisco/Congo craton at 920 Ma. Geological Society, London, Special Publications 424, 167-190.

Evans, M.E., Wayman, M.L., 1974. An Investigation of the Role of Ultra-fine Titanomagnetite Intergrowths in Palaeomagnetism. Geophysical Journal International 36, 1-10.

Fernie, N., Glorie, S., W. Jessell, M., Collins, A., 2018. Thermochronological insights into reactivation of a continental shear zone in response to Equatorial Atlantic rifting (northern Ghana).

Feybesse, J.-L., Billa, M., Guerrot, C., Duguey, E., Lescuyer, J.-L., Milesi, J.-P., Bouchot, V., 2006. The paleoproterozoic Ghanaian province: Geodynamic model and ore controls, including regional stress modeling. Precambrian Research 149, 149-196.

Fisher, R., 1953. Dispersion on a Sphere. Proceedings of the Royal Society of London. Series A. Mathematical and Physical Sciences 217, 295-305.

Fu, X., Zhang, S., Li, H., Ding, J., Li, H., Yang, T., Wu, H., Yuan, H., Lv, J., 2015. New paleomagnetic results from the Huaibei Group and Neoproterozoic mafic sills in the North China Craton and their paleogeographic implications. Precambrian Research 269, 90-106.

Gong, Z., Evans, D.A.D., Elming, S.-Å., Söderlund, U., Salminen, J.M., 2018. Paleomagnetism, magnetic anisotropy and U-Pb baddeleyite geochronology of the early Neoproterozoic Blekinge-Dalarna dolerite dykes, Sweden. Precambrian Research 317, 14-32.

Gower, C., Ryan, A., Rivers, T., 1990. Mid-Proterozoic Laurentia-Baltica: an overview of its geological evolution and a summary of the contributions made by this volume. Mid-Proterozoic Laurentia-Baltica 38, 1-20.

Greenman, J.W., Rainbird, R.H., Turner, E.C., 2020. High-resolution correlation between contrasting early Tonian carbonate successions in NW Canada highlights pronounced global carbon isotope variations. Precambrian Research 346, 105816.

Haggerty, S.E., 1991. Oxide textures; a mini-atlas. Reviews in Mineralogy and Geochemistry 25, 129-219.

Hartz, E.H., Torsvik, T., 2002. Baltica upside down: A new plate tectonic model for Rodinia and the Iapetus Ocean. Geology 30, 255-258.

Heaman, L.M., LeCheminant, A.N., 2001. Anomalous U–Pb systematics in mantle-derived baddeleyite xenocrysts from Île Bizard: evidence for high temperature radon diffusion? Chemical Geology 172, 77-93.

Hoffman, P.F., 1991. Did the breakout of Laurentia turn Gondwanaland inside-out? Science 252, 1409.

Jessell, M., Santoul, J., Baratoux, L., Youbi, N., Ernst, R.E., Metelka, V., Miller, J., Perrouty, S., 2015. An Updated Map of West African Mafic Dykes. Journal of African Earth Sciences 112, 440-450.

Jing, X., Yang, Z., Evans, D.A.D., Tong, Y., Xu, Y., Wang, H., 2019. A pan-latitudinal Rodinia in the Tonian true polar wander frame. Earth and Planetary Science Letters, 115880.

Johansson, Å., 2009. Baltica, Amazonia and the SAMBA connection—1000 million years of neighbourhood during the Proterozoic? Precambrian Research 175, 221-234.

Kalsbeek, F., Frei, D., Affaton, P., 2008. Constraints on provenance, stratigraphic correlation and structural context of the Volta basin, Ghana, from detrital zircon geochronology: An Amazonian connection? Sedimentary Geology 212, 86-95.

Kirschvink, J., 1978. The Precambrian-Cambrian boundary problem: paleomagnetic directions from the Amadeus Basin, central Australia. Earth and Planetary Science Letters 40, 91-100.

Kirschvink, J.L., 1980. The least-squares line and plane and the analysis of palaeomagnetic data. Geophysical Journal International 62, 699-718.

Kirschvink, J.L., Kopp, R.E., Raub, T.D., Baumgartner, C.T., Holt, J.W., 2008. Rapid, precise, and high-sensitivity acquisition of paleomagnetic and rock-magnetic data: Development of a low-noise automatic sample changing system for superconducting rock magnetometers. Geochemistry, Geophysics, Geosystems 9.

Kouyaté, D., Söderlund, U., Youbi, N., Ernst, R., Hafid, A., Ikenne, M., Soulaimani, A., Bertrand, H., El Janati, M.h., R'Kha Chaham, K., 2013. U–Pb baddeleyite and zircon ages of 2040 Ma, 1650 Ma and 885 Ma on dolerites in the West African Craton (Anti-Atlas inliers): Possible links to break-up of Precambrian supercontinents. Lithos 174, 71-84.

Li, Z.-X., Evans, D.A.D., Halverson, G.P., 2013. Neoproterozoic glaciations in a revised global palaeogeography from the breakup of Rodinia to the assembly of Gondwanaland. Sedimentary Geology 294, 219-232.

Li, Z.X., Li, X.H., Kinny, P.D., Wang, J., Zhang, S., Zhou, H., 2003. Geochronology of Neoproterozoic syn-rift magmatism in the Yangtze Craton, South China and correlations with other continents: evidence for a mantle superplume that broke up Rodinia. Precambrian Research 122, 85-109.

Li, Z.X., Evans, D.A.D., Zhang, S., 2004. A 90° spin on Rodinia: possible causal links between the Neoproterozoic supercontinent, superplume, true polar wander and low-latitude glaciation. Earth and Planetary Science Letters 220, 409-421.

Li, Z.X., Bogdanova, S.V., Collins, A.S., Davidson, A., De Waele, B., Ernst, R.E., Fitzsimons, I.C.W., Fuck, R.A., Gladkochub, D.P., Jacobs, J., Karlstrom, K.E., Lu, S., Natapov, L.M., Pease, V., Pisarevsky, S.A., Thrane, K., Vernikovsky, V., 2008. Assembly, configuration, and break-up history of Rodinia: A synthesis. Precambrian Research 160, 179-210.

Li, Z.X., Mitchell, R.N., Spencer, C.J., Ernst, R., Pisarevsky, S., Kirscher, U., Murphy, J.B., 2019. Decoding Earth's rhythms: modulation of supercontinent cycles by longer superocean episodes.

Ludwig, K., 2009. Isoplot 4.1. A geochronological toolkit for Microsoft Excel. Berkeley Geochronology Center Special Publication 4, 76.

Maloof, A.C., Halverson, G.P., Kirschvink, J.L., Schrag, D.P., Weiss, B.P., Hoffman, P.F., 2006. Combined paleomagnetic, isotopic, and stratigraphic evidence for true polar wander from the Neoproterozoic Akademikerbreen Group, Svalbard, Norway. Geological Society of America Bulletin 118, 1099-1124.

Martin, E.L., Spencer, C.J., Collins, W.J., Thomas, R.J., Macey, P.H., Roberts, N.M.W., 2020. The core of Rodinia formed by the juxtaposition of opposed retreating and advancing accretionary orogens. Earth-Science Reviews, 103413.

McDowell, F.W., McIntosh, W.C., Farley, K.A., 2005. A precise 40Ar–39Ar reference age for the Durango apatite (U–Th)/He and fission-track dating standard. Chemical Geology 214, 249-263.

McElhinny, M.W., Powell, C.M., Pisarevsky, S.A., 2003. Paleozoic terranes of eastern Australia and the drift history of Gondwana. Tectonophysics 362, 41-65.

McFadden, P.L., Merrill, R.T., McElhinny, M.W., 1988. Dipole/quadrupole family modeling of paleosecular variation. Journal of Geophysical Research: Solid Earth 93, 11583-11588.

McFadden, P.L., McElhinny, M.W., 1990. Classification of the reversal test in palaeomagnetism. Geophysical Journal International 103, 725-729.

Meert, J.G., Hargraves, R.B., Van der Voo, R., Hall, C.M., Halliday, A.N., 1994a. Paleomagnetic and 40Ar/39Ar studies of Late Kibaran intrusives in Burundi, East Africa: implications for Late Proterozoic supercontinents. The Journal of Geology 102, 621-637.

Meert, J.G., Hargraves, R.B., Van der Voo, R., Hall, C.M., Halliday, A.N., 1994b. Paleomagnetic and Studies of Late Kibaran Intrusives in Burundi, East Africa: Implications for Late Proterozoic Supercontinents. The Journal of Geology 102, 621-637.

Meert, J.G., 2001. Growing Gondwana and Rethinking Rodinia: A Paleomagnetic Perspective. Gondwana Research 4, 279-288.

Meert, J.G., Torsvik, T.H., 2003. The making and unmaking of a supercontinent: Rodinia revisited. Tectonophysics 375, 261-288.

Meert, J.G., 2014. Strange attractors, spiritual interlopers and lonely wanderers: The search for pre-Pangean supercontinents. Geoscience Frontiers 5, 155-166.

Meert, J.G., Pivarunas, A.F., Evans, D.A.D., Pisarevsky, S.A., Pesonen, L.J., Li, Z.-X., Elming, S.-Å., Miller, S.R., Zhang, S., Salminen, J.M., 2020. The magnificent seven: A proposal for modest revision of the Van der Voo (1990) quality index. Tectonophysics 790, 228549.

Merdith, A.S., Collins, A.S., Williams, S.E., Pisarevsky, S., Foden, J.F., Archibald, D., Blades, M.L., Alessio, B.L., Armistead, S., Plavsa, D., Clark, C., Müller, R.D., 2017. A full-plate global reconstruction of the Neoproterozoic. Gondwana Research 50, 84-134.

Mertanen, S., Pesonen, L., Huhma, H., 1996. Palaeomagnetism and Sm-Nd ages of the Neoproterozoic diabase dykes in Laanila and Kautokeino, northern Fennoscandia. Geological Society, London, Special Publications 112, 331-358.

Moores, E.M., 1991. Southwest U.S.-East Antarctic (SWEAT) connection: A hypothesis. Geology 19, 425-428.

Moreira, H.F., Danderfer, A., Costa, A.F.O., Bersan, S.M., Lana, C.C., Queiroga, G.N., 2020. Record of Early Tonian mafic magmatism in the central Espinhaço (Brazil): New insights for break-up of the Neoproterozoic landmass ancestor of São Francisco-Congo paleocontinent. Geoscience Frontiers 11, 2323-2337.

Morris, W., Carmichael, C., 1978. Paleomagnetism of some late Precambrian and lower Paleozoic sediments from L'Adrar de Mauritanie, West Africa. Canadian Journal of Earth Sciences 15, 253-262.

Müller, R.D., Cannon, J., Qin, X., Watson, R.J., Gurnis, M., Williams, S., Pfaffelmoser, T., Seton, M., Russell, S.H.J., Zahirovic, S., 2018. GPlates: Building a Virtual Earth Through Deep Time. Geochemistry, Geophysics, Geosystems 19, 2243-2261.

Murphy, J.B., Nance, R.D., 2003. Do supercontinents introvert or extrovert?: Sm-Nd isotope evidence. Geology 31, 873-876.

Neves, S.P., Teixeira, C.M.L., Bruguier, O., 2020. 870-850 Ma-old magmatic event in eastern Borborema Province, NE Brazil: Another Tonian failed attempt to break up the São Francisco Paleoplate? Journal of South American Earth Sciences, 102917.

Niu, J., Li, Z.-X., Zhu, W., 2016. Palaeomagnetism and geochronology of mid-Neoproterozoic Yanbian dykes, South China: implications for a c. 820–800 Ma true polar wander event

and the reconstruction of Rodinia. Geological Society, London, Special Publications 424, 191-211.

Onstott, T., Hargraves, R.B., 1981. Proterozoic transcurrent tectonics: palaeomagnetic evidence from Venezuela and Africa. Nature 289, 131-136.

Palencia-Ortas, A., Ruiz-Martínez, V.C., Villalaín, J.J., Osete, M.L., Vegas, R., Touil, A., Hafid, A., McIntosh, G., van Hinsbergen, D.J.J., Torsvik, T.H., 2011. A new 200 Ma paleomagnetic pole for Africa, and paleo-secular variation scatter from Central Atlantic Magmatic Province (CAMP) intrusives in Morocco (Ighrem and Foum Zguid dykes). Geophysical Journal International 185, 1220-1234.

Park, J., 1981. Analysis of the multicomponent magnetization of the Little Dal Group, Mackenzie Mountains, Northwest Territories, Canada. Journal of Geophysical Research: Solid Earth 86, 5134-5146.

Patroni, O.A.L., 2015. Estudo Paleomagnético do Complexo Máfico-ultramáfico Rincón del Tigre-Sudeste da Bolívia, Cráton Amazônico, Instituto de Astronomia, Geofísica e Ciências Atmosféricas. Dissertação de Mestrado. Universidade de São Paulo (USP), p. 119.

Perrin, M., Elston, D.P., Moussine-Pouchkine, A., 1988. Paleomagnetism of Proterozoic and Cambrian Strata, Adrar de Mauritanie, CRatonic West Africa. Journal of Geophysical Research: Solid Earth 93, 2159-2178.

Perrin, M., Prévot, M., 1988. Uncertainties about the Proterozoic and Paleozoic polar wander path of the West African craton and Gondwana: evidence for successive remagnetization events. Earth and Planetary Science Letters 88, 337-347.

Pesonen, L.J., Elming, S.Å., Mertanen, S., Pisarevsky, S., D'Agrella-Filho, M.S., Meert, J.G., Schmidt, P.W., Abrahamsen, N., Bylund, G., 2003. Palaeomagnetic configuration of continents during the Proterozoic. Tectonophysics 375, 289-324.

Piper, J.D.A., Lomax, K., 1973. Palaeomagnetism of Precambrian Birrimian and Tarkwaian Rocks of West Africa. Geophysical Journal International 34, 435-450.

Piper, J.D.A., 2007. The Neoproterozoic supercontinent Palaeopangaea. Gondwana Research 12, 202-227.

Pisarevsky, S.A., Natapov, L.M., 2003. Siberia and Rodinia. Tectonophysics 375, 221-245.

Pisarevsky, S.A., Wingate, M.T.D., Powell, C.M., Johnson, S., Evans, D.A.D., 2003. Models of Rodinia assembly and fragmentation. Geological Society, London, Special Publications 206, 35-55.

Robert, B., Besse, J., Blein, O., Greff, M., Baudin, T., Lopes, F., Meslouh, S., Belbadaoui, M., 2017. Constraints on the Ediacaran Inertial Interchange True Polar Wander Hypothesis: a New Paleomagnetic Study in Morocco (West African Craton). Precambrian Research 295, 90-116.

Roberts, A.P., Heslop, D., Zhao, X., Pike, C.R., 2014. Understanding fine magnetic particle systems through use of first-order reversal curve diagrams. Reviews of Geophysics 52, 557-602.

Rooney, A.D., Selby, D., Houzay, J.-P., Renne, P.R., 2010. Re–Os geochronology of a Mesoproterozoic sedimentary succession, Taoudeni basin, Mauritania: Implications for basin-wide correlations and Re–Os organic-rich sediments systematics. Earth and Planetary Science Letters 289, 486-496.

Sadowski, G.R., Bettencourt, J.S., 1996. Mesoproterozoic tectonic correlations between eastern Laurentia and the western border of the Amazon Craton. Precambrian Research 76, 213-227.

Salminen, J., Pesonen, L.J., Mertanen, S., Vuollo, J., Airo, M.-L., 2009. Palaeomagnetism of the Salla Diabase Dyke, northeastern Finland, and its implication for the Baltica-

Laurentia entity during the Mesoproterozoic. Geological Society, London, Special Publications 323, 199-217.

Salminen, J., Mertanen, S., Evans, D.A.D., Wang, Z., 2014. Paleomagnetic and geochemical studies of the Mesoproterozoic Satakunta dyke swarms, Finland, with implications for a Northern Europe – North America (NENA) connection within Nuna supercontinent. Precambrian Research 244, 170-191.

Salminen, J., Hanson, R., Evans, D.A.D., Gong, Z., Larson, T., Walker, O., Gumsley, A., Söderlund, U., Ernst, R., 2018. Direct Mesoproterozoic connection of the Congo and Kalahari cratons in proto-Africa: Strange attractors across supercontinental cycles. Geology.

Samson, S.D., Inglis, J.D., D'Lemos, R.S., Admou, H., Blichert-Toft, J., Hefferan, K., 2004. Geochronological, geochemical, and Nd–Hf isotopic constraints on the origin of Neoproterozoic plagiogranites in the Tasriwine ophiolite, Anti-Atlas orogen, Morocco. Precambrian Research 135, 133-147.

Sears, J.W., Price, R.A., 1978. The Siberian Connection: A case for Precambrian separation of the North American and Siberian cratons. Geology 6, 267-270.

Sears, J.W., Price, R.A., 2000. New look at the Siberian connection: No SWEAT. Geology 28, 423-426.

Stacey, J.S., Kramers, J.D., 1975. Approximation of terrestrial lead isotope evolution by a two-stage model. Earth and Planetary Science Letters 26, 207-221.

Stearn, J.E.F., Piper, J.D.A., 1984. Palaeomagnetism of the Sveconorwegian mobile belt of the Fennoscandian Shield. Precambrian Research 23, 201-246.

Swanson-Hysell, N.L., Maloof, A.C., Kirschvink, J.L., Evans, D.A.D., Halverson, G.P., Hurtgen, M.T., 2012. Constraints on Neoproterozoic paleogeography and Paleozoic orogenesis from paleomagnetic records of the Bitter Springs Formation, Amadeus Basin, central Australia. American Journal of Science 312, 817-884.

Swanson-Hysell, N.L., Kilian, T.M., Hanson, R.E., 2015a. A new grand mean palaeomagnetic pole for the 1.11 Ga Umkondo large igneous province with implications for palaeogeography and the geomagnetic field. Geophysical Journal International 203, 2237-2247.

Swanson-Hysell, N.L., Maloof, A.C., Condon, D.J., Jenkin, G.R.T., Alene, M., Tremblay, M.M., Tesema, T., Rooney, A.D., Haileab, B., 2015b. Stratigraphy and geochronology of the Tambien Group, Ethiopia: Evidence for globally synchronous carbon isotope change in the Neoproterozoic. Geology 43, 323-326.

Swanson-Hysell, N.L., Ramezani, J., Fairchild, L.M., Rose, I.R., 2019. Failed rifting and fast drifting: Midcontinent rift development, Laurentia's rapid motion and the driver of Grenvillian orogenesis. Bulletin 131, 913-940.

Teixeira, W., Hamilton, M.A., Lima, G.A., Ruiz, A.S., Matos, R., Ernst, R.E., 2015. Precise ID-TIMS U–Pb baddeleyite ages (1110–1112 Ma) for the Rincón del Tigre–Huanchaca large igneous province (LIP) of the Amazonian Craton: Implications for the Rodinia supercontinent. Precambrian Research 265, 273-285.

Terentiev, R.A., Santosh, M., 2020. Baltica (East European Craton) and Atlantica (Amazonian and West African Cratons) in the Proterozoic: The pre-Columbia connection. Earth-Science Reviews 210, 103378.

Thompson, J., Meffre, S., Maas, R., Kamenetsky, V., Kamenetsky, M., Goemann, K., Ehrig, K., Danyushevsky, L., 2016. Matrix effects in Pb/U measurements during LA-ICP-MS analysis of the mineral apatite. Journal of Analytical Atomic Spectrometry 31, 1206-1215.

Thomson, S.N., Gehrels, G.E., Ruiz, J., Buchwaldt, R., 2012. Routine low-damage apatite U-Pb dating using laser ablation–multicollector–ICPMS. Geochemistry, Geophysics, Geosystems 13.

Tohver, E., van der Pluijm, B.A., Van der Voo, R., Rizzotto, G., Scandolara, J.E., 2002. Paleogeography of the Amazon craton at 1.2 Ga: early Grenvillian collision with the Llano segment of Laurentia. Earth and Planetary Science Letters 199, 185-200.

Tohver, E., D'Agrella-Filho, M.S., Trindade, R.I.F., 2006. Paleomagnetic record of Africa and South America for the 1200–500 Ma interval, and evaluation of Rodinia and Gondwana assemblies. Precambrian Research 147, 193-222.

Triantafyllou, A., Berger, J., Baele, J.-M., Diot, H., Ennih, N., Plissart, G., Monnier, C., Watlet, A., Bruguier, O., Spagna, P., Vandycke, S., 2016. The Tachakoucht–Iriri–Tourtit arc complex (Moroccan Anti-Atlas): Neoproterozoic records of polyphased subduction-accretion dynamics during the Pan-African orogeny. Journal of Geodynamics 96, 81-103.

van Acken, D., Thomson, D., Rainbird, R.H., Creaser, R.A., 2013. Constraining the depositional history of the Neoproterozoic Shaler Supergroup, Amundsen Basin, NW Canada: Rhenium-osmium dating of black shales from the Wynniatt and Boot Inlet Formations. Precambrian Research 236, 124-131.

Vandamme, D., 1994. A new method to determine paleosecular variation. Physics of the Earth and Planetary Interiors 85, 131-142.

Vicat, J.P., Pouclet, A., 1995. Nature du magmatisme lie a une extension pre-panafricaine; les dolerites des bassins de Comba et de Sembe-Ouesso (Congo). Bulletin de la Société Géologique de France 166, 355-364.

Walderhaug, H.J., Torsvik, T.H., Eide, E.A., Sundvoll, B., Bingen, B., 1999. Geochronology and palaeomagnetism of the Hunnedalen dykes, SW Norway: implications for the Sveconorwegian apparent polar wander loop. Earth and Planetary Science Letters 169, 71-83.

Walderhaug, H.J., Torsvik, T.H., Halvorsen, E., 2007. The Egersund dykes (SW Norway): A robust early Ediacaran (Vendian) palaeomagnetic pole from Baltica. Geophysical Journal International 168, 935-948.

Wen, B., Evans, D.A., Wang, C., Li, Y.-X., Jing, X., 2018. A positive test for the Greater Tarim Block at the heart of Rodinia: Mega-dextral suturing of supercontinent assembly. Geology.

Wiedenbeck, M., Alle, P., Corfu, F., Griffin, W., Meier, M., Oberli, F.v., Quadt, A.v., Roddick, J., Spiegel, W., 1995. Three natural zircon standards for U- Th- Pb, Lu- Hf, trace element and REE analyses. Geostandards newsletter 19, 1-23.

Wingate, M.T.D., Pisarevsky, S.A., Evans, D.A.D., 2002. Rodinia connections between Australia and Laurentia: no SWEAT, no AUSWUS? Terra Nova 14, 121-128.

Zijderveld, J., 1967. AC demagnetization of rocks: analysis of results. Methods in paleomagnetism 3, 254.

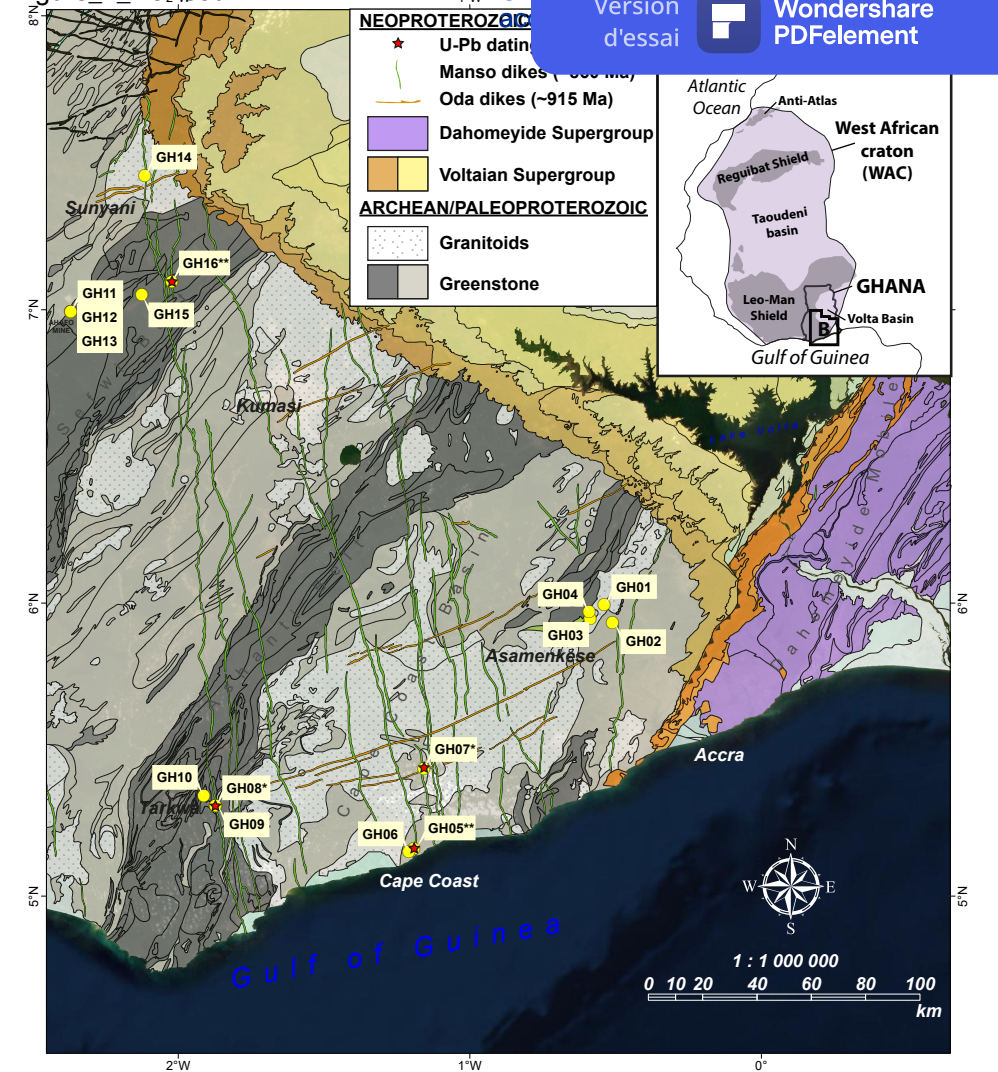

Figure 1

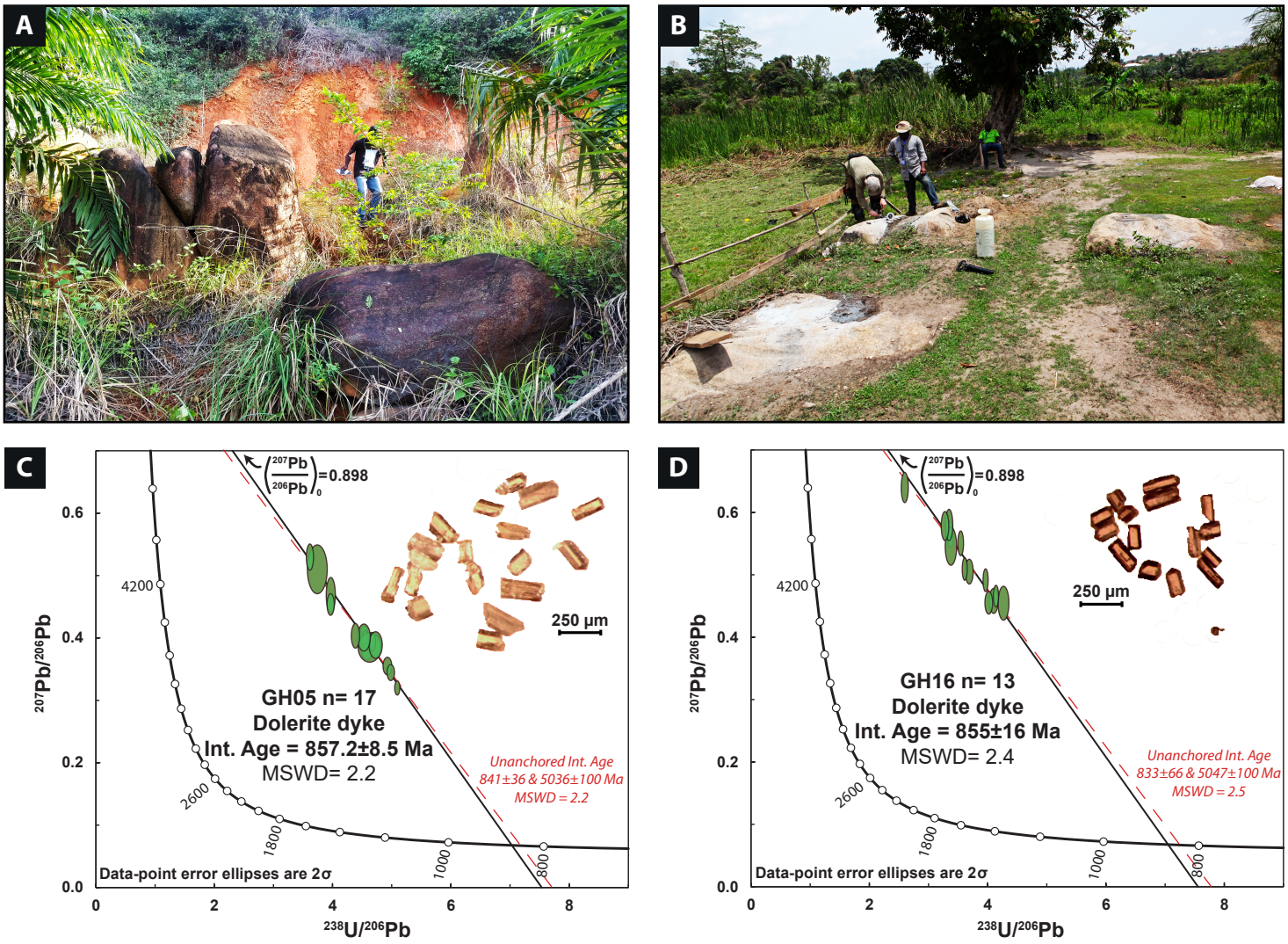

Figure 2

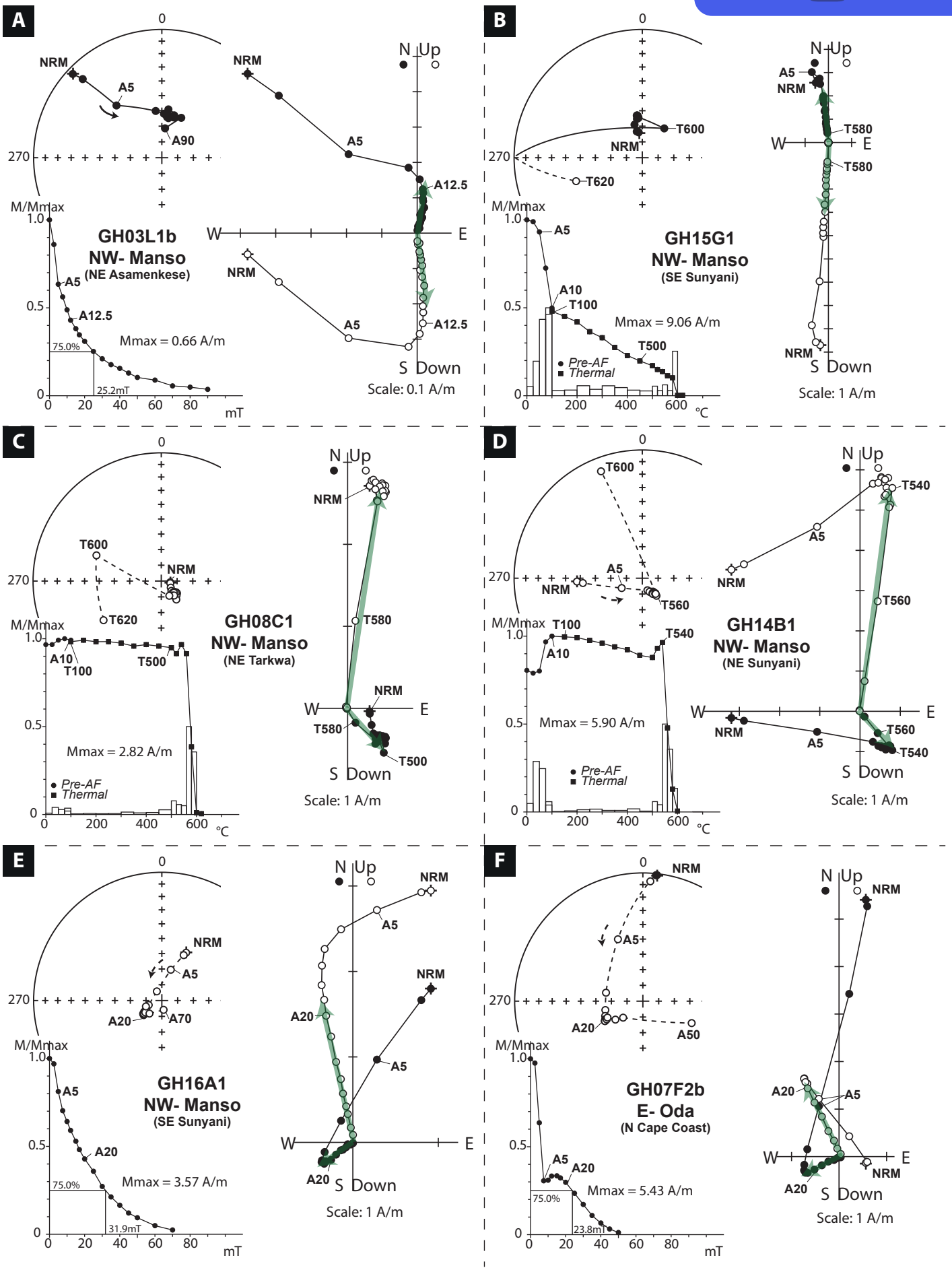

Figure 3

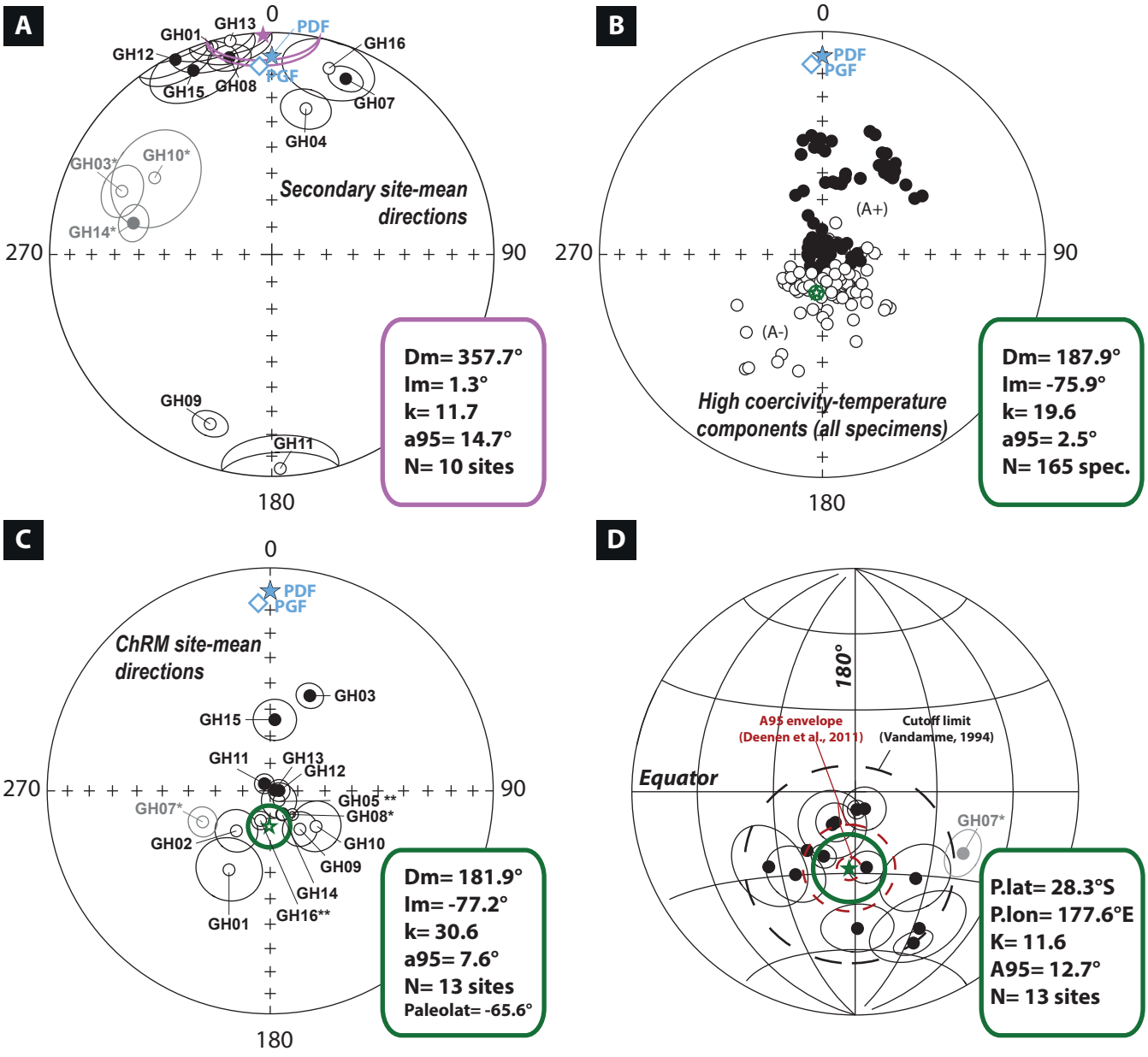

Figure 4

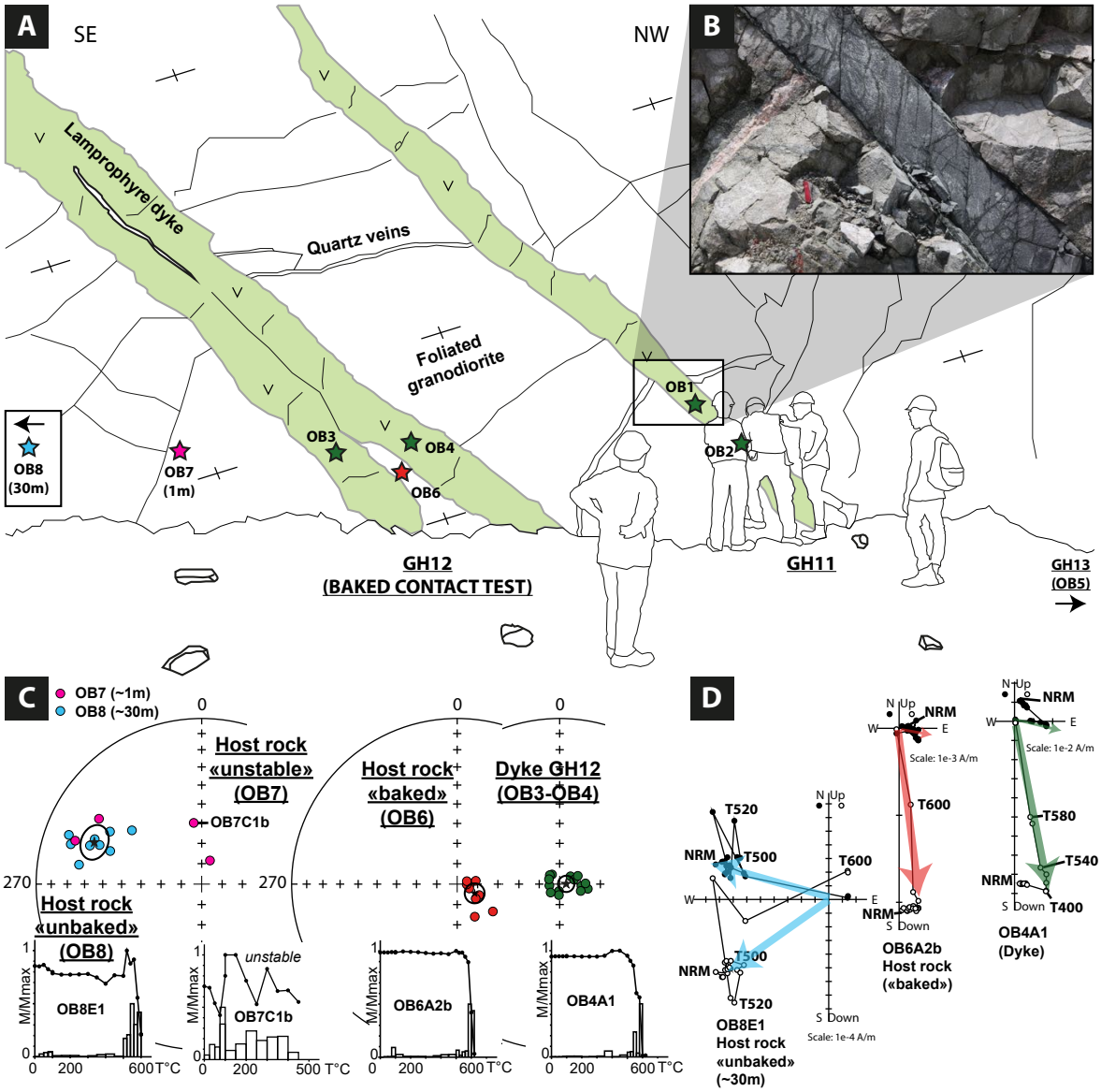

Figure 5

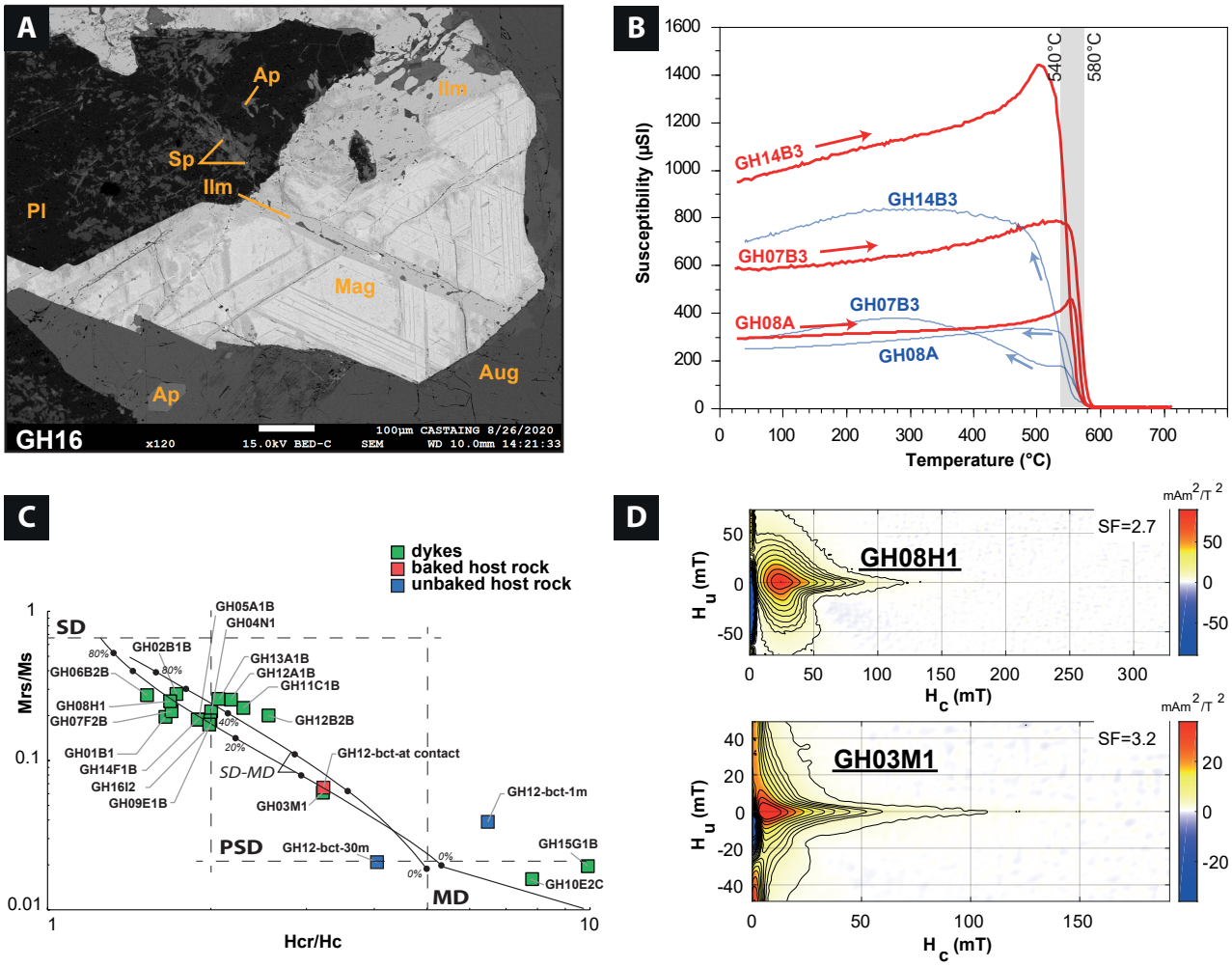

Figure 6

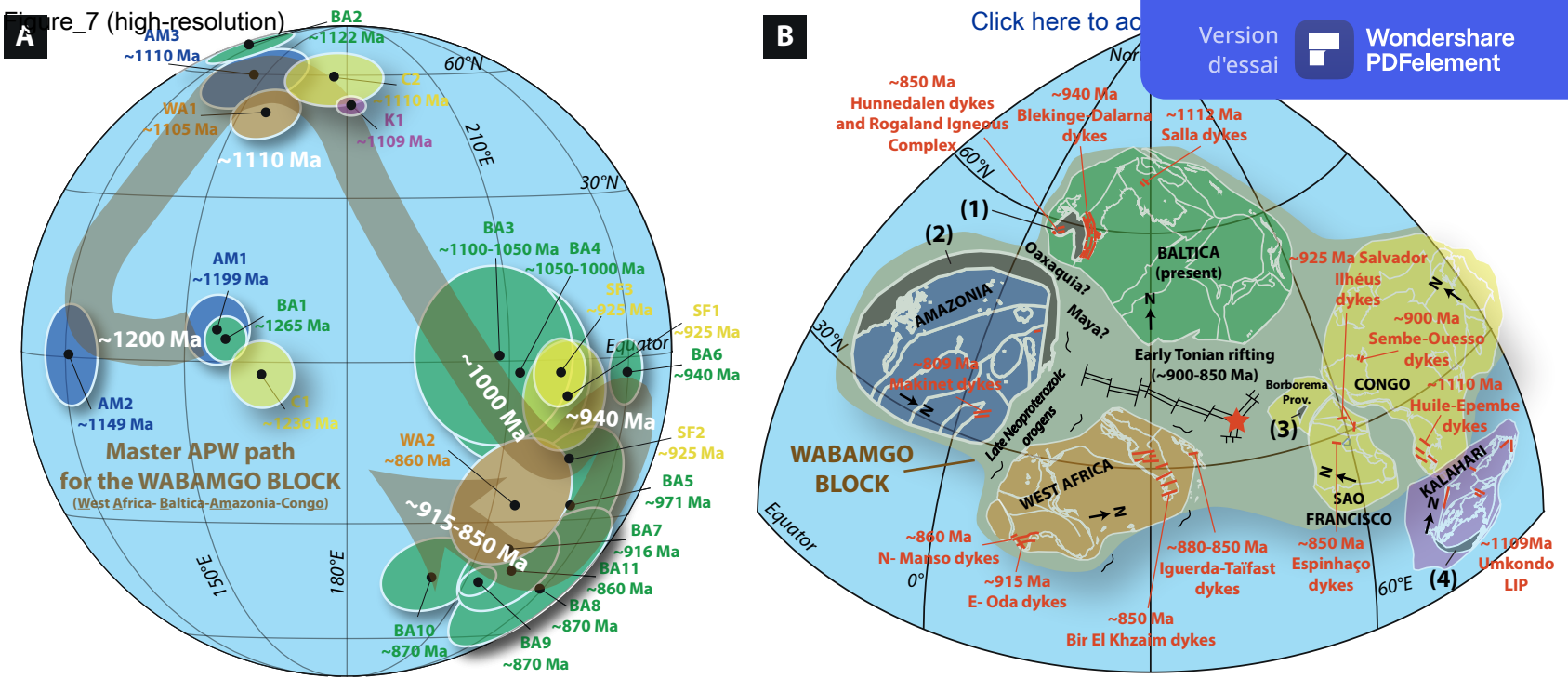

Figure 7

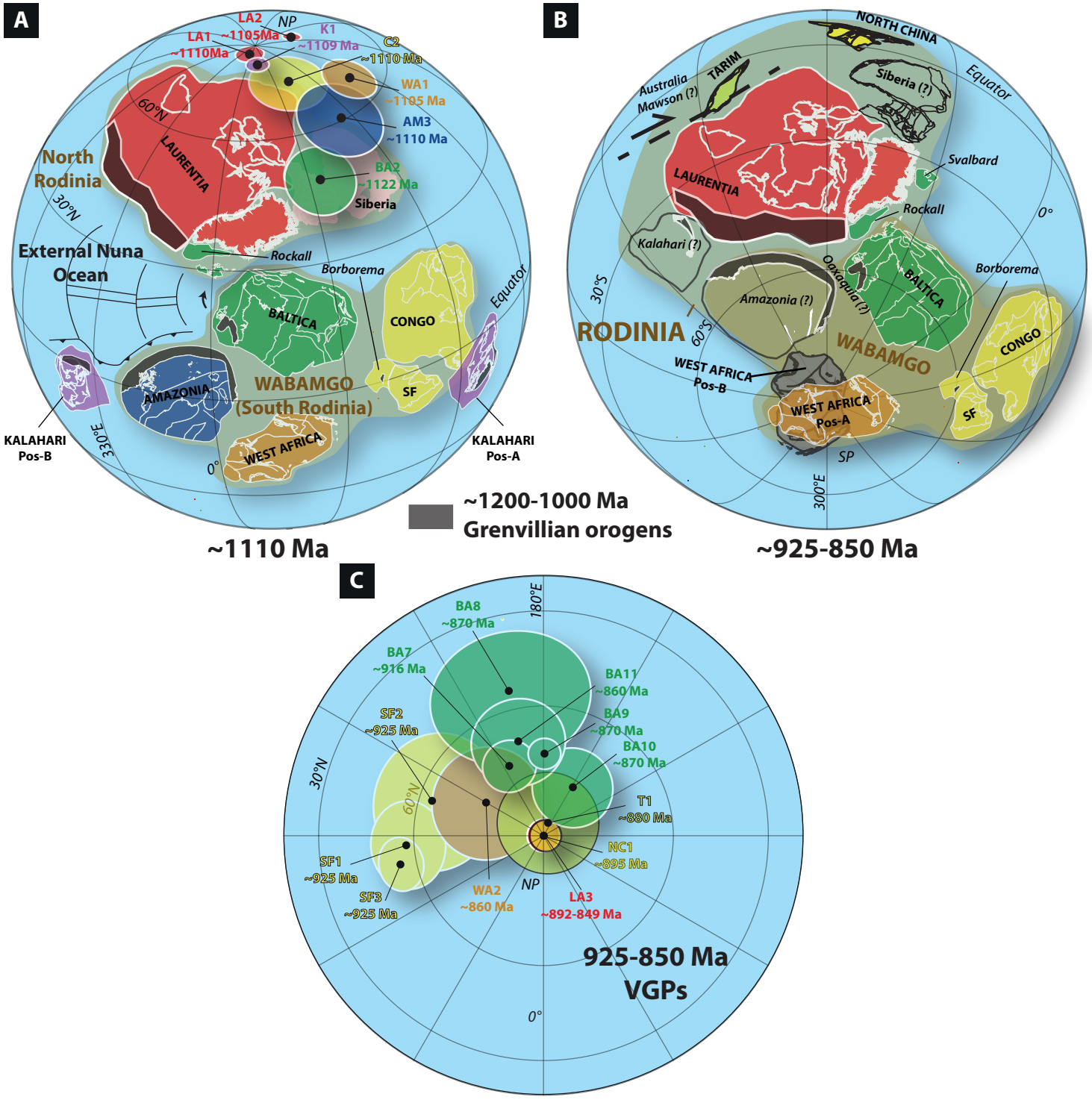

Figure 8